

REPORT

***NUMERICAL MODELING OF LONG-TERM PERMAFROST DYNAMICS OF THE
KINIKTUURAQ PROPOSED RELOCATION SITE FOR THE COMMUNITY OF KIVALINA***

***KIVALINA TOWNSITE RELOCATION
KIVALINA, ALASKA***

Prepared for:

**Federal Highway Administration
Western Federal Lands Highway Division**

Prepared by:

**Permafrost Lab
Geophysical Institute
University of Alaska Fairbanks**

August, 2008

Project Location.

Kivalina is located at latitude 67° 44' N, longitude 164° 33' W approximately 80 miles (mi) north of the Arctic Circle on the Chukchi Sea coast of northwestern Alaska. Kivalina is 74 mi northwest of Kotzebue. The community is located at the southeastern tip of an 8-mile barrier spit that separates Kivalina Lagoon from the Chukchi Sea. Kivalina is on an island defined by two tidal inlets: Singauk Inlet at the southeast end of the island and Kivalik Inlet, 5.5 mi to the northwest. The Kivalina River empties into Kivalina Lagoon at its northern extreme, and the Wulik River empties into the lagoon at its southern extreme. Kivalina is located in the Kotzebue Recording District. The community boundary encompasses 1.9 square miles of land and 2.0 square miles of water. The community lies in the transitional climate zone characterized by long, cold winters and cool summers. The average low temperature during January is -15° F; the average high temperature during July is 57° F. Temperature extremes have been measured from -54 to 85° F. Snowfall averages 57 inches, with 8.6 inches of precipitation per year. Travel to Kivalina is accomplished by sea, or by small plane from Kotzebue. Snow machines provide limited access to the community during the winter. The Chukchi Sea has historically been ice-free and open to boat traffic from early July to late October. The village is 80 air miles northwest of Kotzebue and approximately 18 miles up the coast from the Red Dog Mine port site.

Project Background.

Kivalina, population 377, is a traditional Iñupiat Eskimo village. Like the other Arctic Ocean communities, subsistence hunting, fishing, and gathering, including whaling, provide most of the community's foods. The communities in the region rely on the coast for many of their most important resources, and there is a long history of human occupation. In recent years, a combination of reduced ice protection on shore and a longer fetch for storm waves out of the northwest have combined to accelerate coastal erosion throughout the region. In Kivalina, the fall storms have become major threats to village infrastructure and safety. Kivalina, Shishmaref, and other communities in the region are exploring the steps needed to relocate to higher ground near existing community sites. While relocating is in the planning stage, preliminary design for an evacuation road to high ground must begin immediately. To the extent practical, a road would take into consideration the selected new village site, needed material sites, and other elements for successful village relocation. The subject of overall project is preliminary engineering to investigate the feasibility and location of an evacuation road that the community could use to access high ground during storm events. One possible village relocation site is Kiniktuuraq. To better evaluate this site, a Long Term Permafrost Dynamic Model is requested. The scope of this sub-project is as follows:

Project Long-Term Permafrost Dynamics Scope:

1. Develop a numerical model for long-term permafrost dynamics at this site. Model should take in consideration the present-day climate, soil properties, and ground surface conditions. The model should include the freezing/thawing processes and unfrozen water dynamics. Climate and soil conditions should be derived from existing reports and other available information.
2. Make several simulations for the period 2005-2050 using the developed model for three different thicknesses of gravel fill (6, 9, and 12 feet thick) positioned directly on the existing natural surface and for three different climate scenarios (conservative, moderate, and extreme in terms of future warming). Repeat simulations for the case with fine-grained fill (silt) with 1-foot gravel cap on top of the fine-grained fill.

Model description.

In order to assess possible changes in the permafrost thermal state and the active layer depth, the GIPL-2.0 (Geophysical Institute Permafrost Lab) model was used (Marchenko, et al., 2008). The GIPL-2.0 model numerically simulates soil temperature dynamics and the depth of seasonal freezing and thawing by solving 1D non-linear heat equation with phase change. In this model the process of soil freezing/thawing is occurring in accordance with the volumetric unfrozen water content curve and soil thermal properties, which are specific for each soil layer at the specific site. Unfrozen water content was parameterized by power function $Q(T)=A*(T_{fr}-T)^B$, where $A>0$, $B<0$, T is soil temperature, and T_{fr} is a temperature of the beginning of phase changes (liquid water to ice) in soil. Special Enthalpy formulation of the energy conservation law makes it possible to use a coarse vertical resolution without loss of latent heat effects in phase transition zone even in case of fast temporally varying temperature fields. The input data for the model are air temperature from observations or climate forcing from Global or Regional Climate Models, soils properties, vegetation, and snow cover properties (depth, density, thermal conductivity). The new version of GIPL-2.0 simulates soil temperature and liquid water content fields for the entire calculated period with daily, monthly and yearly resolution.

The spatial irregular grid for the simulations contained 252 grid points with the vertical spatial interval of 0.01 m for the upper part of the simulated domain increasing to 0.05, 0.5, 1.0 and 5 m toward the lower boundary that was located at 100 m depth. The upwards geothermal flux applied at the base (100 m depth) of the soil domain was set to be 0.02 W/m^2 .

The soil characterization used in the GIPL-2.0 model is based on data derived from the existing report on geotechnical investigation conducted by R&M Consulting Inc. for the U.S. Army Engineer District Alaska (Report. R&M Consultants, Inc. August, 2002).

Monthly variations of the insulating effect of snow cover on ground temperatures are modeled explicitly by adding/removing snow layers on top of the calculation domain in accordance with snow accumulation/melt. The temperature of the snow surface and the air temperature are assumed to be equal (Andersland & Ladanyi, 2004). The snow properties were prescribed by assuming a snow density dependence on snow water equivalent and air temperature.

Mathematical model

The basic mathematical model in our approach is the Enthalpy formulation of the one-dimensional Stefan problem (Alexiades & Solomon 1993, Verdi 1994). We used the quasi-linear heat conduction equation, which expresses the energy conservation law:

$$\frac{\partial H(y,t)}{\partial \tau} = \text{div}(\lambda(y,t)\nabla t(y,\tau)), y \in \Omega, \tau \in \Psi \quad (1)$$

where $H(y, t)$ is the enthalpy

$$H(y,t) = \int_0^t C(y,s)ds + L\Theta(y,t) \quad (2)$$

$C(y, t)$ is the heat capacity, L is the latent heat, $\lambda(y, \tau)$ is thermal conductivity and $\Theta(y, t)$ is the volumetric unfrozen water content. The Equation (1) is complemented with boundary and initial conditions. The computational domain $-2 \leq \Omega \leq 100$ m extended to 100 m in depth, and time interval Ψ is 102 years (1948-2050) with initial temporal step of 24 hours. Monthly snow cover are modeled explicitly by adding or removing points in the vertical grid $[-2, 0]$ above 0 m (surface) level in accordance with snow accumulation or melting.

Dirichlet's conditions $t(\tau)$ were set at the upper boundary. An empirical method of geothermal heat flux estimating (Pollack et al. 1993) was applied for the lower boundary conditions.

$$\left. \frac{\partial t}{\partial \tau} \right|_{y=0} = t(\tau), \quad \left. \frac{\partial t(\tau)}{\partial y} \right|_{y=100} = g \quad (3)$$

where g is a geothermal gradient at the lower boundary.

A fractional step approach (Godunov splitting) was used to obtain a finite difference scheme (Marchuk 1975). The idea is to divide each time step into two steps. At each step along the spatial dimension (in the depth) is treated implicitly:

$$\begin{aligned} \frac{H(t_i^{n+1}) - H(t_i^{n+1/2})}{\Delta \tau_n} &= \frac{2}{(\Delta h_{i+1} + \Delta h_i)} \\ &\times \left(\lambda_{i+1/2}^{n+1} \frac{(t_{i+1}^{n+1} - t_i^{n+1})}{\Delta h_{i+1,y}} - \lambda_{i-1/2}^{n+1} \frac{(t_i^{n+1} - t_{i-1}^{n+1})}{\Delta h_{i,y}} \right) \end{aligned} \quad (4)$$

where $\Delta h_{i,y}$ is the spatial steps on the non-uniform grid.

The resulting system of finite difference equations is non-linear, and to solve it, the Newton's method was employed at each time step. On the first half step (4) in case when a non-zero gradient of temperature exist, we use the difference derivative of enthalpy:

$$\frac{\partial H(t_i)}{\partial t} = 0.5 \left[\frac{H(t_i) - H(t_{i-1})}{(t_i - t_{i-1})} + \frac{H(t_{i+1}) - H(t_i)}{(t_{i+1} - t_i)} \right] \quad (5)$$

The analytical derivative of representation (2) has to be used in case of zero-gradient temperature fields. Second half step (4) is treated similarly. Thereby, we can employ any size spatial steps without any risk to lose any latent heat effects within the phase transition zone for the fast temporally varying temperature fields.

Model validation and calibration.

Ground temperature measurements in boreholes obtained by R&M Consultants, Inc were used for initial model validation. Air temperature and snow depth recorded in Kivalina during Nov 1973 - Nov 1975 has a very good correlation with the long term series observed in Kotzebue weather station. The correlation coefficients between two data sets are 0.97 for the air temperature series and 0.88 for snow depth.

The soil thermal conductivity and heat capacity vary within the different soil layers as well as during the thawing/freezing cycles and depend on the unfrozen water content that is a certain function of temperature. The method of obtaining these properties is based on numerical solution for a coefficient inverse problem and on minimization locally the misfit between measured and modeled temperatures by changing thermal properties along the direction of the steepest descent (Nicolsky et al., 2007).

The model calibration was performed for the Kiniktuuraq AP-06 specific site (Figures 1-2) with further simulation of permafrost dynamics for the period of continuous climate observations during 1948-2007 (Figures 3-6).

Climate forcing.

For the geothermal reanalysis during 1948-2007 (Figures 3-6) at the Kiniktuuraq AP-06 proposed relocation site we used data on air temperature (Figure 6a) and snow depth and duration (Figure 6b) from the Kotzebue weather station adapted to the Kivalina site.

As a climate forcing for the period 2008-2050 we used output data from the Coupled Global Climate Model (CGCM3), which is the third generation of the Canadian Center for Climate Modeling and Analysis (CCCma) CGCM3 (Boer et al., 2000 a, b; Boer et al., 1992; Flato et al., 2000; Web: http://www.cccma.ec.gc.ca/eng_index.shtml). CGCM3 couples the atmospheric model to a specially adapted version of the GFDL Modular Ocean Model and a thermodynamic sea-ice model. Output data from the simulations have been contributed to the IPCC Data Distribution Center to facilitate its use for climate impact studies. This model has also been used for the US National Assessment.

An ensemble of four transient climate change simulations has been performed and is described in Boer et al. (2000). Three of these simulations use an effective greenhouse gas forcing change corresponding to that observed from 1850 to 1990, and a forcing change corresponding to an increase of CO₂ at a rate of 1% per year (compounded) thereafter until year 2100 (the IPCC IS92a forcing scenario).

For the permafrost change projections we used two different scenarios. The **A1B** scenario is a more aggressive scenario with increase of mean annual air temperature by approximately 4°C by the end of the 21st century. The **B1** scenario is a more conservative with increasing in air temperature by about 2°C towards the end of the 21st century.

Model runs.

In order to assess possible changes in the permafrost thermal state and the active layer depth, the eighteen GIPL-2.0 model runs were performed for the Kiniktuuraq AP-06 proposed relocation site using different combinations of the upper boundary conditions and soil properties.

1. Natural conditions.

Five model runs were performed in order to assess the permafrost dynamics at the Kiniktuuraq AP-06 proposed relocation site for natural (undisturbed) conditions. One model run was implemented for historical period 1948-2007 (Figures 3-6). Other four runs were performed according to CGCM3 scenarios for the period 2008-2050 (Figures 7-12). Figures 7, 8, and 9 illustrate the result of projected mean annual soil temperature dynamics at the Kiniktuuraq AP-06 site during 2008-2050. These two runs used CGCM3 **A1B** and **B1** output in terms of air temperature and snow cover depth. Other two runs (Figures 10, 11, 12) were performed using the CGCM3 **A1B** and **B1** output for the air temperature and historical data on the snow depth observed at the Kotzebue weather station and adapted to the Kivalina site. The snow records from 1965-2007 were simply repeated for 2008-2050.

2. Gravel fill.

Figure 13 shows the CCCma CGCM3 forcing, which have been used for the simulations of permafrost temperature dynamics for the case with modified surface conditions (gravel fill and silt + gravel cap) at the Kiniktuuraq AP-06 proposed relocation site during 2008-2050. The **A1B** scenario (Figure 13 left) is a more aggressive scenario with increase of mean annual air temperature by approximately 4°C by the end of the 21st century. The **B1** scenario (Figure 13 right) is more conservative with increase in air temperature by about 2°C towards the end of the 21st century.

We performed six simulations for the period 2008-2050 for 6, 9, and 12 feet (1.82, 2.74, and 3.66 m) thick layers of gravel fill positioned directly on the existing natural surface and for two different climate scenarios derived from CGCM3. Surface energy transfer at the air-ground surface interface

during the period without snow cover and with mean monthly air temperatures above 0°C is described by using the n-factor method ([Ref to](#)). Figures 14-22 illustrate the results of these six different model runs.

3. Fine-grained fill (silt) with 1-foot gravel cap.

The next six simulations were performed for the fine-grained fill (silt) 5, 8, and 11 feet (1.5, 2.42, and 3.34 m) thick with 1-foot gravel cap on top of the fine-grained fill (Figures 23-31).

4. Additional model run

The last model run was performed for the warmest case with CGCM3 **A1B** forcing and gravel fill 12 feet (3.65 m) thick. This special model run simulated snow cover removing. In this run, it is supposed that snow has been removed immediately after each snowfall and snow cover at the top of the gravel fill had never exceeded 0.1 m in depth. Snow cover removing allows avoiding insulating effect of snow and more effective ground cooling during the wintertime. Results of this simulation are shown in Figure 32b.

Summary of the obtained results

We compared result of GIPL ground temperature simulations for two **A1B** and **B1** CCCma CGCM3 scenarios of air temperature and snow depth evolution during 2008-2050. According to lithologic column obtained from the AP-06 site (Figure 2a) the ice-bearing horizon located between 0.4-1.0 m. The frozen state of this ice-rich permafrost layer could be considered as a criterion of the gravel or silt fill stability. A major threshold will be crossed when permafrost thaws down to this layer and the melting ice will cause the surface subsidence. This critical depth is shown as a line on 2D time-depth temperature field diagrams (Figures 15, 16, 18, 19 etc).

1. Effect of Different Climate Scenarios. The way in which the climate will change in the near future plays the main role in the stability of permafrost under the artificial fills. Even for the same natural conditions we can have very different results using different scenario of air temperature and snow cover changes (Figures 8-12). The thawing depth could increase up to 1.5 m between 2025 and 2030 and reach 2 m in depth by 2047 in accordance with **A1B** scenario (Figure 8). The thawing does not penetrate through the ice-rich permafrost horizon according to **B1** scenario (Figure 9). The result could be more dramatic under **A1B** scenario in combination with thicker snow cover observed at the nearest weather station Kotzebue during 1965 – 2007 (Figure 11).

2. Effect of a Gravel fill. According to simulations, the different thicknesses of gravel fill could delay for some time the thawing penetration into the icy layer, but could not completely protect the icy layer from thawing. Thus, the stable thawing process within the ice bearing layer under **A1B** climate scenario probably could start after 7-8 years of gravel fill placement for the case with 6 ft gravel pad (Figure 15), after 10-11 years for the case with 9 ft gravel pad (Figure 18), and after 12-13 years for the case with 12 ft/3.66 m gravel pad (Figure 21). Complete thawing of the very ice-rich permafrost layer takes approximately 5-10 years depending on the gravel fill thickness (Figures 15, 18, 21). Even more conservative **B1** scenario could lead to a partial (Figure 19, 22) or complete (Figure 16) thawing of this very ice-rich permafrost layer and to penetration of the thawing front into the ice-rich permafrost beneath. According to the modeling results using the **A1B** scenario, increase in the gravel fill thickness from 6 to 12 feet (1.8 m to 3.66 m) leads to insignificant decrease in the thawing penetration into the underlying ice-rich soils from about 1.8-2 m beneath the gravel fill (Figure 15) to approximately 1.4-1.5 m for the case with 12 ft/3.66 m gravel fill thickness by 2050 (Figure 21). In both cases under this climate scenario, the very ice-rich permafrost layer

thawed completely. Under the more conservative **B1** scenario of climate warming, the thickness of the gravel fill probably may play a significant role in determining if the very ice-rich permafrost layer will thawed completely (Figure 16) or just partially by 2050 (Figures 9, 22).

3. Effect of a Fine-grained fill (silt) with 1-foot gravel cap. Numerical simulations of the heat transfer within the fine-grained soil show that this type of fills is generally more protective in terms of permafrost stability in comparison with the gravel fills. However, this effect depends on the chosen climate scenario. Increasing of fine-grained fill from 5 to 11 ft (1.5 to 3.35 m) with 1 f/0.3 m gravel cap had effect for the case with **B1** scenario (Figure 25, 31). While under more aggressive **A1B** scenario, increasing in the fill thickness resulted in just a delay in time when the ice-rich permafrost degradation started and in duration of time required for the complete thawing of the very ice-rich soil layer (Figures 24, 30). Moreover, the fine-grained soils are prone to frost heaving.

4. Snow factor. As it shown in Figures 32 and 33, the snow insulation is one of the dominant factors for permafrost thermal state stability. It could be the most effective way to preserve permafrost if a significant snow accumulation at the top of the fills could be avoided by complete or even partial removal of the snow from the fill surfaces.

Soil thermal properties.

For simulations the lithologic cross-section from the AP-06 borehole was used (Figure 2). The soil thermal properties which been using for simulations shown in Table 1.

- NUM - number of the soil layer;
 - VWC - volumetric water content;
 - CAPth - heat capacity thawed [J/(m³*K)];
 - CAPfr - heat capacity frozen [J/(m³*K)];
 - Kth - thermal conductivity thawed [W/(m*K)];
 - Kfr - thermal conductivity frozen [W/(m*K)];
 - A - A-factor for the unfrozen water curve;
 - B - B-power factor for the unfrozen water curve;
- Unfrozen Water content: $Q(T)=A*(T_{fr}-T)^B$, where $A>0$, $B<0$ and T_{fr} is the temperature of fusion

Table 1. Soil thermal properties.

NUATURAL CONDITIONS									
NUM	VWC	CAPth	CAPfr	Kth	Kfr	A	B	Layer Depth	
1	0.58	2.1e6	1.7e6	0.32	2.12	0.03	-0.3	0.0-0.12 m / MOSS	
2	0.62	2.1e6	1.7e6	0.52	2.22	0.03	-0.3	0.12-0.6 m / PEAT & ICE + PEAT	
3	0.68	2.5e6	2.0e6	1.05	2.25	0.04	-0.2	0.6-0.9 m / ICE + SILT	
4	0.48	2.5e6	1.7e6	1.35	1.98	0.01	-0.25	0.9-7.1 m / SILT	
5	0.36	2.6e6	2.1e6	1.8	2.5	0.03	-0.5	7.1-50 m / GRAVEL	
6	0.15	2.7e6	2.6e6	2.4	2.55	0.01	-0.7	50.0-100 m / BEDROCK	
GRAVEL 6 ft / 1.8 m									
NUM	VWC	CAPth	CAPfr	Kth	Kfr	A	B	Layer Depth	
1	0.18	2.6e6	2.1e6	1.45	1.95	0.03	-0.35	0.0-1.8 m / GRAVEL	
2	0.58	2.1e6	1.7e6	0.32	2.12	0.03	-0.3	1.8-1.92 m / MOSS	
3	0.62	2.1e6	1.7e6	0.52	2.22	0.03	-0.3	1.92-2.4 m / PEAT & ICE + PEAT	
4	0.68	2.5e6	2.0e6	1.05	2.25	0.04	-0.2	2.4-2.7 m / ICE + SILT	
5	0.48	2.5e6	1.7e6	1.35	1.98	0.01	-0.25	2.7-8.9 m / SILT	
6	0.36	2.6e6	2.1e6	1.8	2.5	0.03	-0.5	8.9-51.8 m / GRAVEL	
7	0.15	2.7e6	2.6e6	2.4	2.55	0.01	-0.7	51.8-100 m / BEDROCK	
GRAVEL 9 ft / 2.74 m									

NUM	VWC	CAPth	CAPfr	Kth	Kfr	A	B	Layer Depth	
1	0.18	2.6e6	2.1e6	1.45	1.95	0.03	-0.35	0.0-2.75	m / GRAVEL
2	0.58	2.1e6	1.7e6	0.32	2.12	0.03	-0.3	2.75-2.87	m / MOSS
3	0.62	2.1e6	1.7e6	0.52	2.22	0.03	-0.3	2.87-3.35	m / PEAT & ICE + PEAT
4	0.68	2.5e6	2.0e6	1.05	2.25	0.04	-0.2	3.35-3.65	m / ICE + SILT
5	0.48	2.5e6	1.7e6	1.35	1.98	0.01	-0.25	3.65-9.85	m / SILT
6	0.36	2.6e6	2.1e6	1.8	2.5	0.03	-0.5	9.85-52.75	m / GRAVEL
7	0.15	2.7e6	2.6e6	2.4	2.55	0.01	-0.7	52.75-100	m / BEDROCK
GRAVEL 12 ft / 3.66 m									
NUM	VWC	CAPth	CAPfr	Kth	Kfr	A	B	Layer Depth	
1	0.18	2.6e6	2.1e6	1.45	1.95	0.03	-0.35	0.0-2.75	m / GRAVEL
2	0.58	2.1e6	1.7e6	0.32	2.12	0.03	-0.3	2.75-2.87	m / MOSS
3	0.62	2.1e6	1.7e6	0.52	2.22	0.03	-0.3	2.87-3.35	m / PEAT & ICE + PEAT
4	0.68	2.5e6	2.0e6	1.05	2.25	0.04	-0.2	3.35-3.65	m / ICE + SILT
5	0.48	2.5e6	1.7e6	1.35	1.98	0.01	-0.25	3.65-9.85	m / SILT
6	0.36	2.6e6	2.1e6	1.8	2.5	0.03	-0.5	9.85-52.75	m / GRAVEL
7	0.15	2.7e6	2.6e6	2.4	2.55	0.01	-0.7	52.75-100	m / BEDROCK
SILT+GRAVEL 5+1 ft / 1.5+0.3 m									
NUM	VWC	CAPth	CAPfr	Kth	Kfr	A	B	Layer Depth	
1	0.18	2.6e6	2.1e6	1.45	1.95	0.03	-0.35	0.0-0.3	m / GRAVEL
2	0.48	2.5e6	1.7e6	1.25	1.98	0.01	-0.25	0.3-1.8	m / SILT
3	0.58	2.1e6	1.7e6	0.32	2.12	0.03	-0.3	1.8-1.92	m / MOSS
4	0.62	2.1e6	1.7e6	0.52	2.22	0.03	-0.3	1.92-2.4	m / PEAT & ICE + PEAT
5	0.68	2.5e6	2.0e6	1.05	2.25	0.04	-0.2	2.4-2.7	m / ICE + SILT
6	0.48	2.5e6	1.7e6	1.35	1.98	0.01	-0.25	2.7-8.9	m / SILT
7	0.36	2.6e6	2.1e6	1.8	2.5	0.03	-0.5	8.9-51.8	m / GRAVEL
8	0.15	2.7e6	2.6e6	2.4	2.55	0.01	-0.7	51.8-100	m / BEDROCK
SILT+GRAVEL 8+1 ft / 2.45+0.3 m									
NUM	VWC	CAPth	CAPfr	Kth	Kfr	A	B	Layer Depth	
1	0.18	2.6e6	2.1e6	1.45	1.95	0.03	-0.35	0.0-0.3	m / GRAVEL
2	0.48	2.5e6	1.7e6	1.25	1.98	0.01	-0.25	0.3-2.75	m / SILT
3	0.58	2.1e6	1.7e6	0.32	2.12	0.03	-0.3	2.75-2.87	m / MOSS
4	0.62	2.1e6	1.7e6	0.52	2.22	0.03	-0.3	2.87-3.35	m / PEAT & ICE + PEAT
5	0.68	2.5e6	2.0e6	1.05	2.25	0.04	-0.2	3.35-3.65	m / ICE + SILT
6	0.48	2.5e6	1.7e6	1.35	1.98	0.01	-0.25	3.65-9.85	m / SILT
7	0.36	2.6e6	2.1e6	1.8	2.5	0.03	-0.5	9.85-52.75	m / GRAVEL
8	0.15	2.7e6	2.6e6	2.4	2.55	0.01	-0.7	52.75-100	m / BEDROCK
SILT+GRAVEL 11+1 ft / 3.35+0.3 m									
NUM	VWC	CAPth	CAPfr	Kth	Kfr	A	B	Layer Depth	
1	0.18	2.6e6	2.1e6	1.45	1.95	0.03	-0.35	0-0.3	m / GRAVEL
2	0.48	2.5e6	1.7e6	1.25	1.98	0.01	-0.25	0.3-3.65	m / SILT
3	0.58	2.1e6	1.7e6	0.32	2.12	0.03	-0.3	3.65-3.77	m / MOSS
4	0.62	2.1e6	1.7e6	0.52	2.22	0.03	-0.3	3.77-4.25	m / PEAT & ICE + PEAT
5	0.68	2.5e6	2.0e6	1.05	2.25	0.04	-0.2	4.25-4.55	m / ICE + SILT
6	0.48	2.5e6	1.7e6	1.35	1.98	0.01	-0.25	4.55-10.75	m / SILT
7	0.36	2.6e6	2.1e6	1.8	2.5	0.03	-0.5	10.75-53.65	m / GRAVEL
8	0.15	2.7e6	2.6e6	2.4	2.55	0.01	-0.7	53.65-100	m / BEDROCK

References

- Alexiades, V. and Solomon, A. D. 1993. Mathematical modeling of melting and freezing processes, Washington, Hemisphere, 325 pp.
- Andersland, O.B. and Ladanyi, B. 2004. Frozen ground engineering, 2nd edition, John Wiley & Sons.
- Boer, G.J., Flato, G.M, and Ramsden, D., 2000b: A transient climate change simulation with historical and projected greenhouse gas and aerosol forcing: projected climate for the 21st century. *Climate Dynamics*, 16, 427-450.
- Boer, G.J., Flato, G.M., Reader, M.C., and Ramsden, D., 2000a: A transient climate change simulation with historical and projected greenhouse gas and aerosol forcing: experimental design and comparison with the instrumental record for the 20th century. *Climate Dynamics*, 16, 405-425.
- Boer, G.J., N.A. McFarlane, and M. Lazare, 1992: Greenhouse Gas-induced Climate Change Simulated with the CCC Second-Generation General Circulation Model. *J. Climate*, 5, 1045-1077.
- Flato, G.M., Boer, G.J., Lee, W.G., McFarlane, N.A., Ramsden, D., Reader, M.C., and Weaver, A.J., 2000: The Canadian Centre for Climate Modelling and Analysis Global Coupled Model and its Climate. *Climate Dynamics*, 16, 451-467.
- Marchenko, S., Romanovsky, V. & Tipenko, G. 2008. Numerical Modeling of Spatial Permafrost Dynamics in Alaska. Proceedings of the Ninth International Conference on Permafrost, Kane DL & Hinkel KM (eds), Institute of Northern Engineering, University of Alaska Fairbanks, Jun 29 - July 3, 2008, 2: 1125-1130.
- Marchuk, G.I. 1975. *Methods of Numerical Mathematics (Applications of Mathematics)*. New York, Springer-Verlag, 316 pp.
- Nicolsky, D. J., Romanovsky, V.E., and G. S.Tipenko, Using in-situ temperature measurements to estimate saturated soil thermal properties by solving a sequence of optimization problems, *The Cryosphere*, 1, 41–58, 2007.
- Report. Phase II Engineering Seervices Geotechnical Investigation. Kivalina Townsite Relocation Kivalina, Alaska. R&M Consultants, Inc. August, 2002.
- Verdi, C. 1994. Numerical aspects of parabolic free boundary and hysteresis problems. *Lecture Notes in Mathematics*, New York, Springer-Verlag, 213-284.

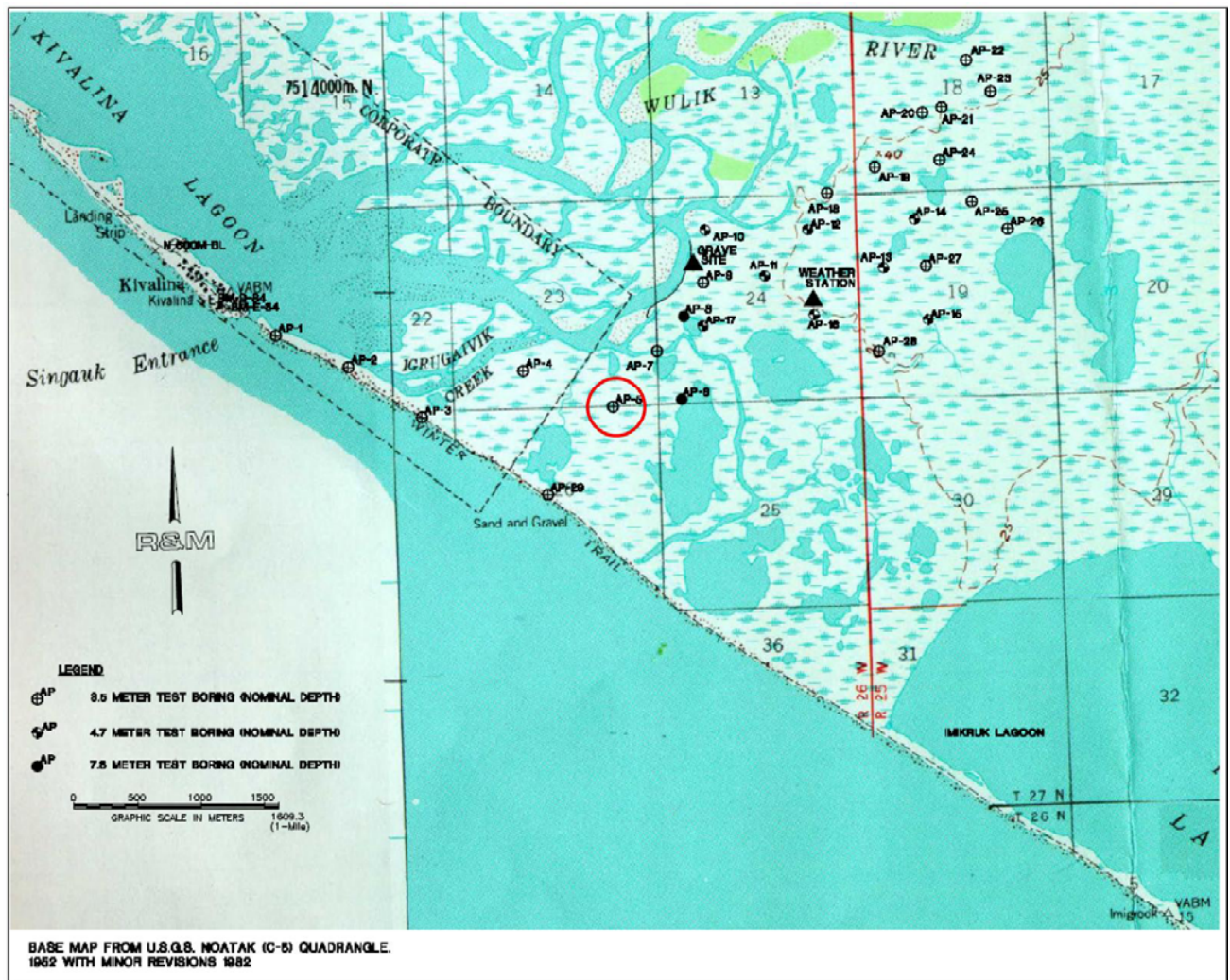


Figure 1. Location of the boreholes where soil core samples were obtained by R&M Consultants Inc (Report. R&M Consultants, Inc. August, 2002). Soil temperature measurements also were made in several boreholes. A red circle marks AP-06 borehole.

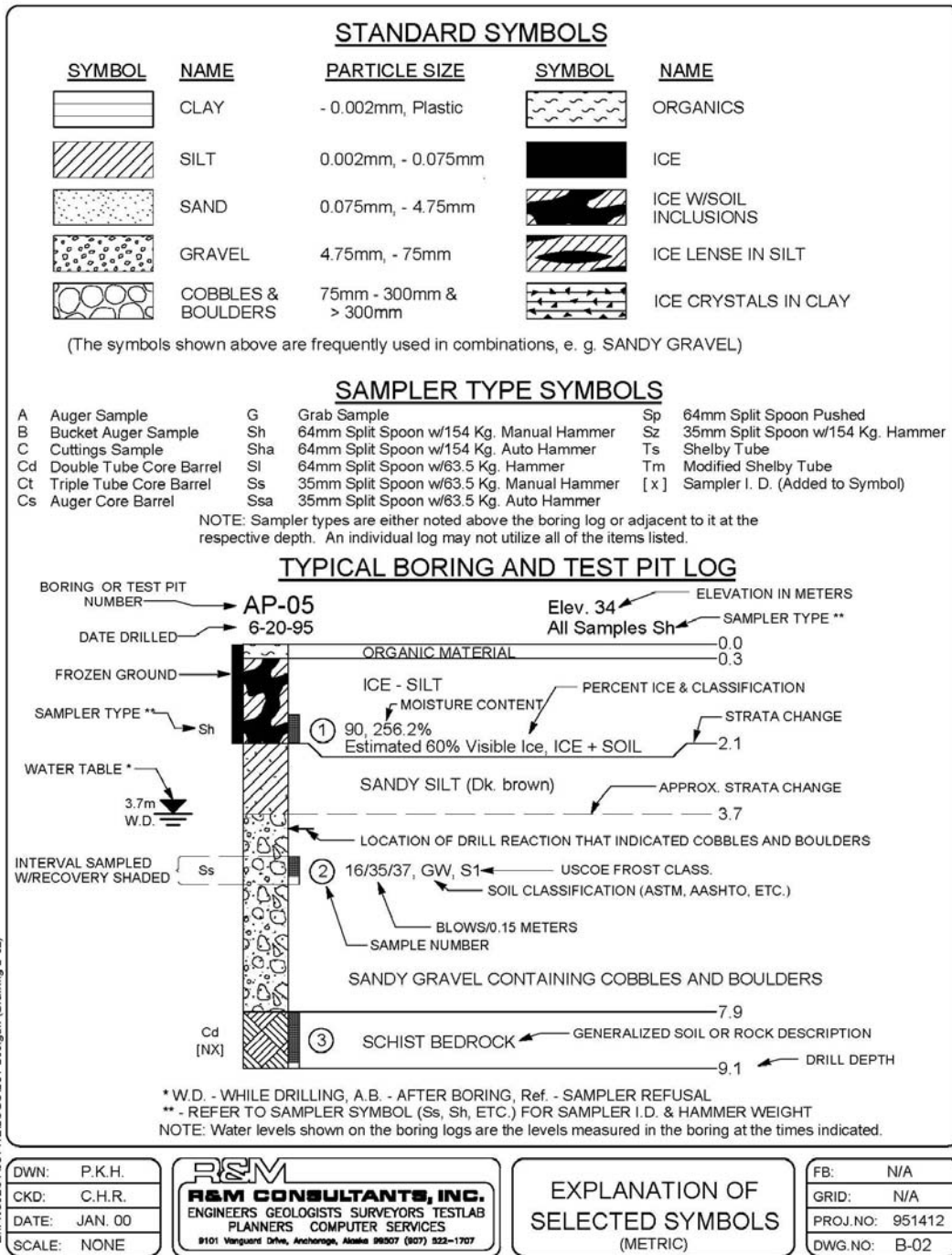


Figure 2. Symbols used for lithology column (Report. R&M Consultants, Inc. August, 2002).

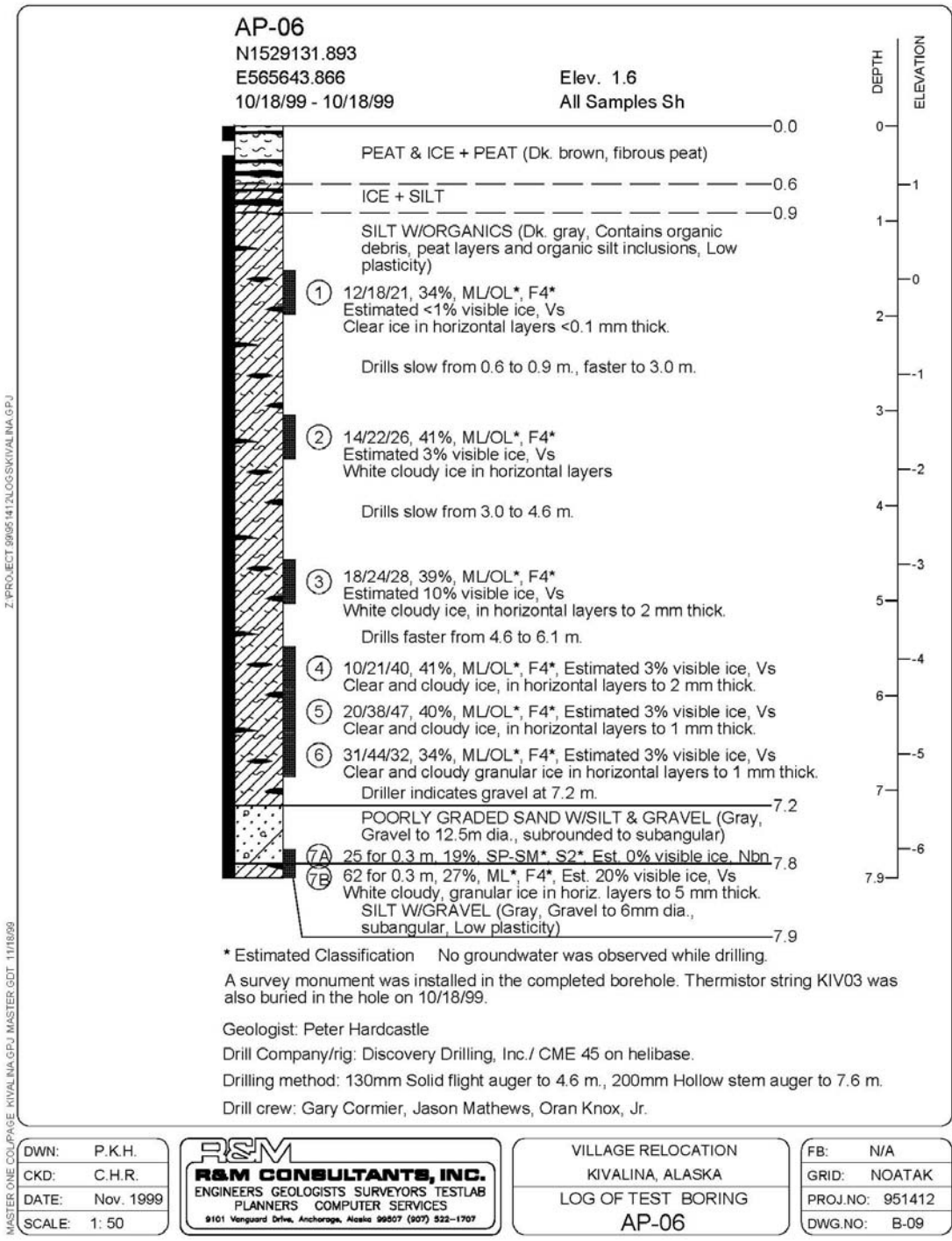


Figure 2a. Lithology of the Kinikturaq AP-06 proposed relocation site used as input data (Report. R&M Consultants, Inc. August, 2002).

Geothermal Reanalysis 1948-2007

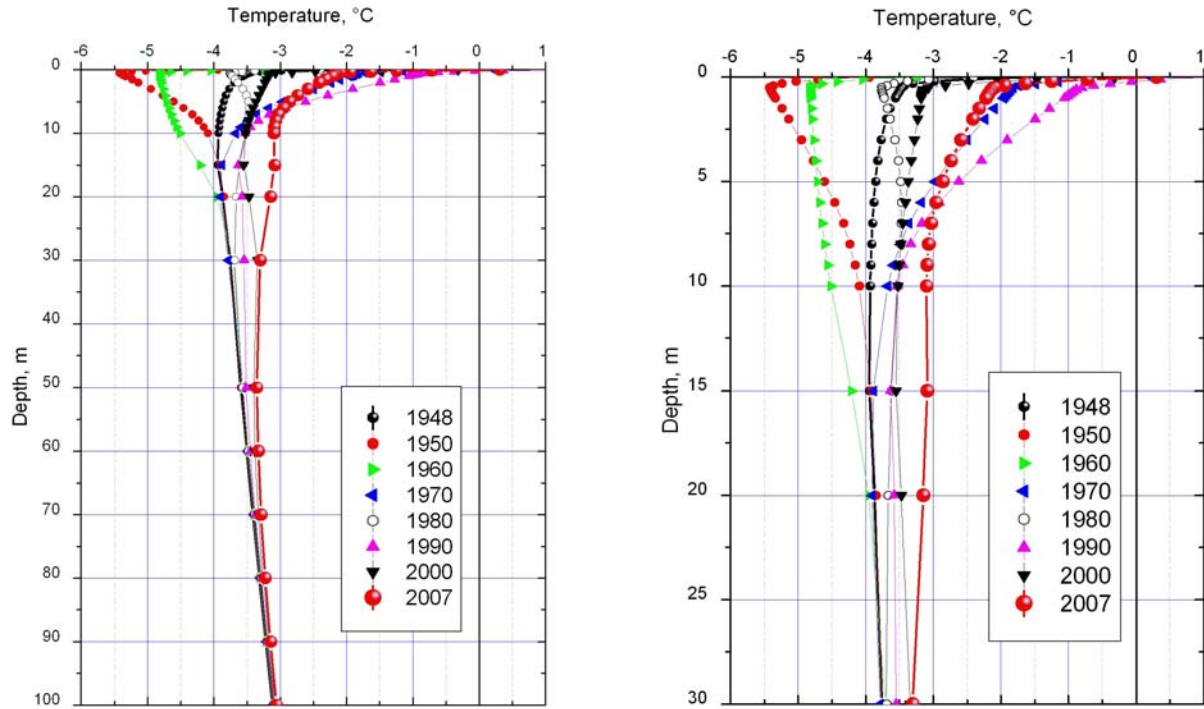


Figure 3. Modeled distribution of mean annual soil temperature with depth for the Kiniktuuraq AP-06 proposed relocation site for the period 1948-2007.

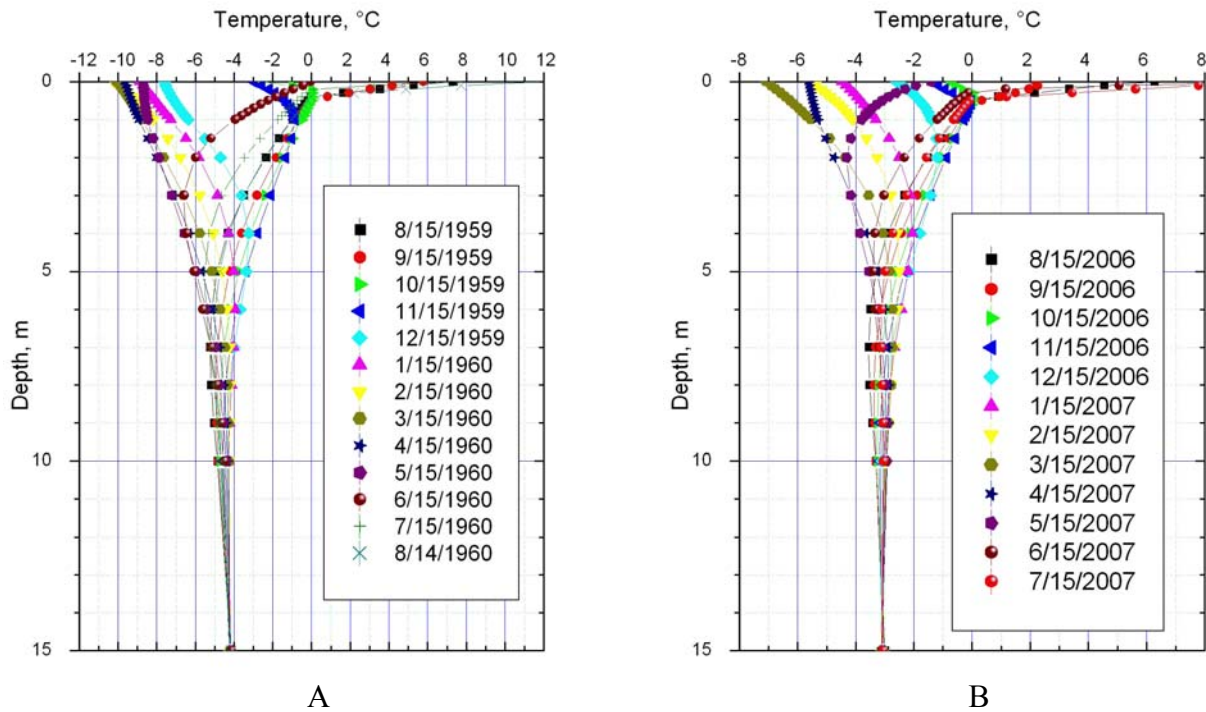


Figure 4. Seasonal variations of soil temperature at the Kiniktuuraq AP-06 proposed relocation site in 1959-60 (A) and 2006-07 (B).

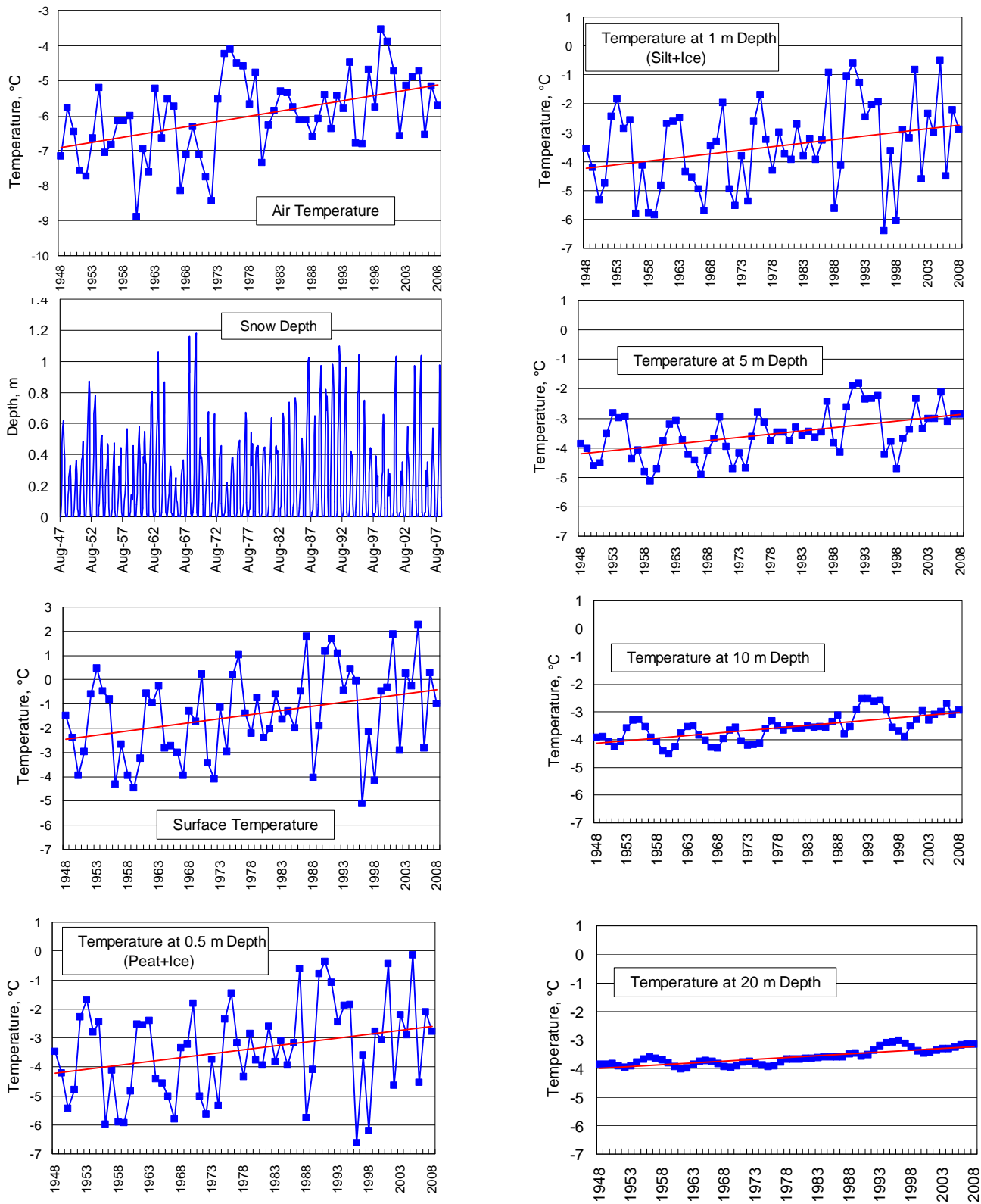


Figure 5. Time series of mean annual air temperature and snow depth together with modeled mean annual permafrost temperatures at different depths for the Kiniktuuraq AP-06 proposed relocation site during 1948-2008.

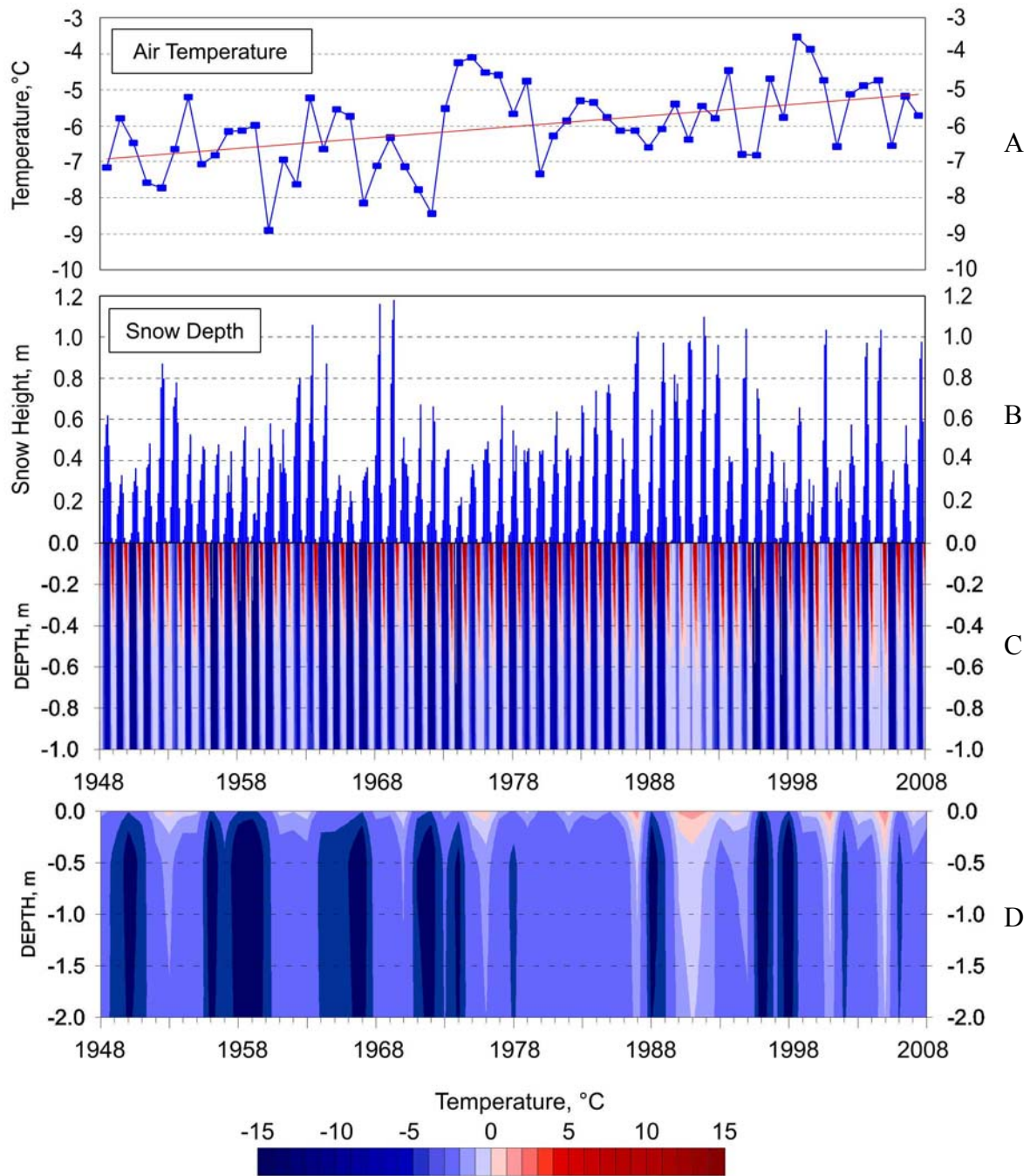


Figure 6. Mean annual air temperature change (A), snow cover (B), and modeled seasonal (C) and annual (D) 2D soil temperature field dynamics for the Kiniktuaraq AP-06 proposed relocation site during 1948-2008.

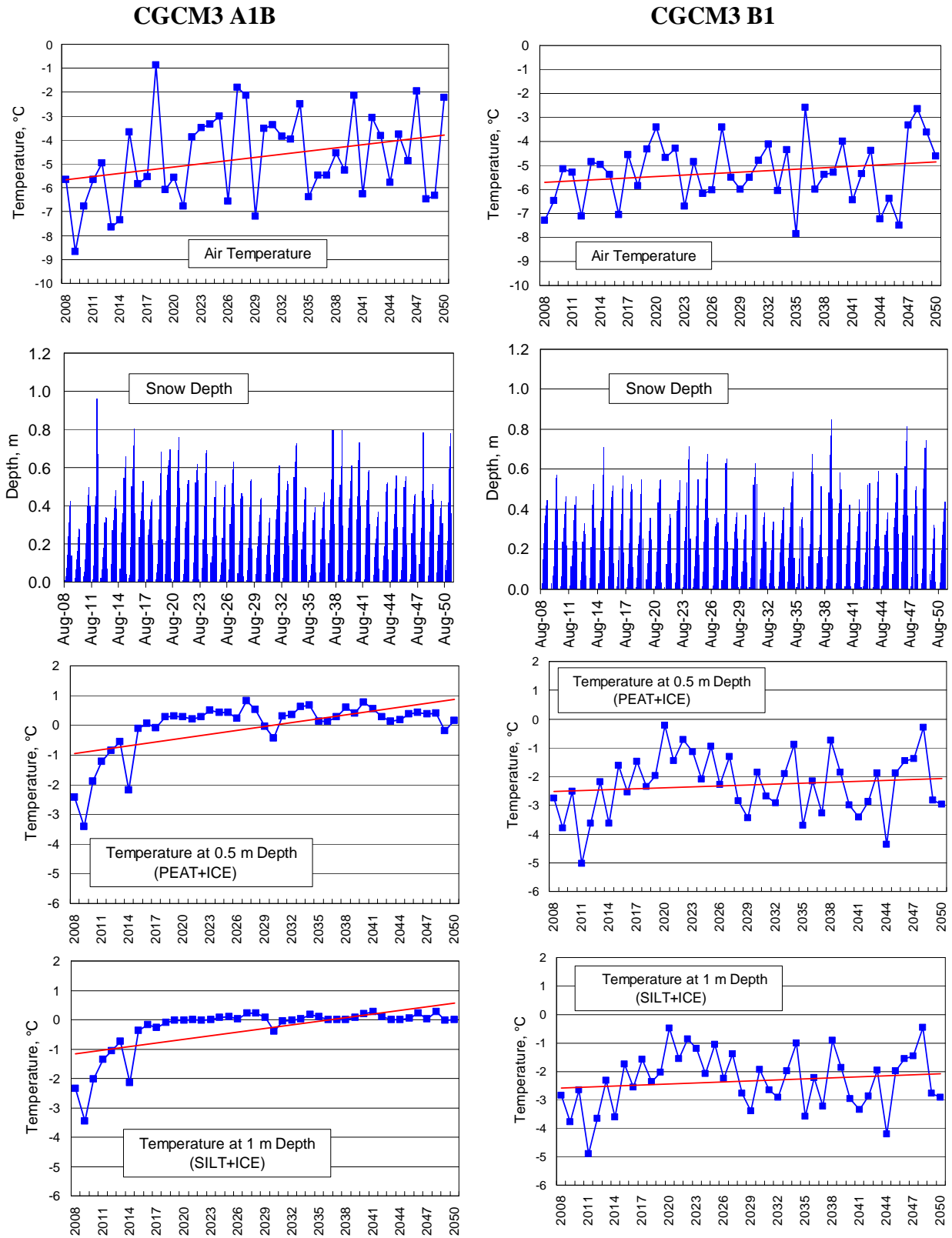


Figure 7. Modeled (CCCma CGCM3) mean annual air temperature and snow depth and modeled (GIPL) soil temperature dynamics for the natural conditions at the Kiniktuaraq AP-06 proposed relocation site during 2008-2050 using CCCma CGCM3 **A1B** and **B1** forcing scenario.

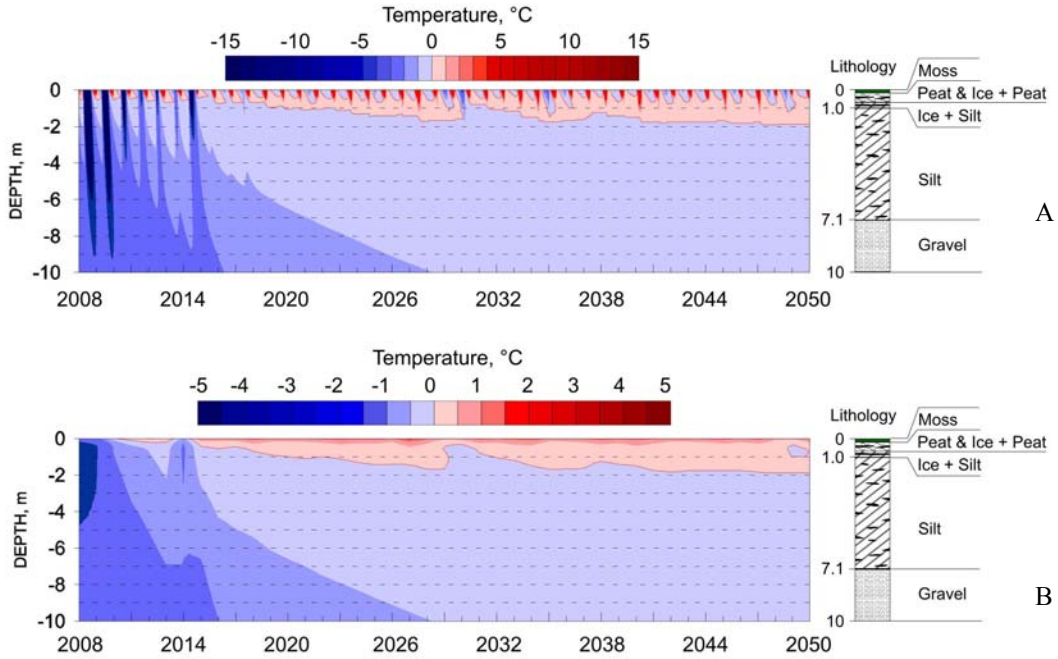


Figure 8. Modeled seasonal (A) and mean annual (B) permafrost temperature field dynamics for the natural conditions at the Kiniktuaraq AP-06 proposed relocation site during 2008-2050 using CCCma CGCM3 **A1B** forcing scenario.

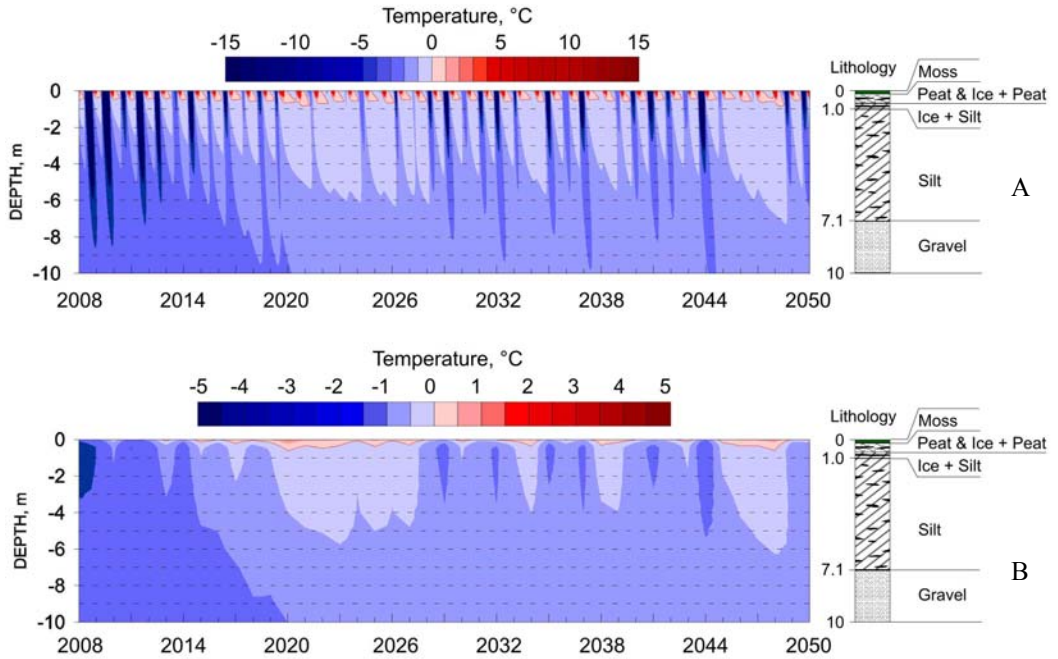


Figure 9. Modeled seasonal (A) and mean annual (B) permafrost temperature field dynamics for the natural conditions at the Kiniktuaraq AP-06 proposed relocation site during 2008-2050 using CCCma CGCM3 **B1** forcing scenario.

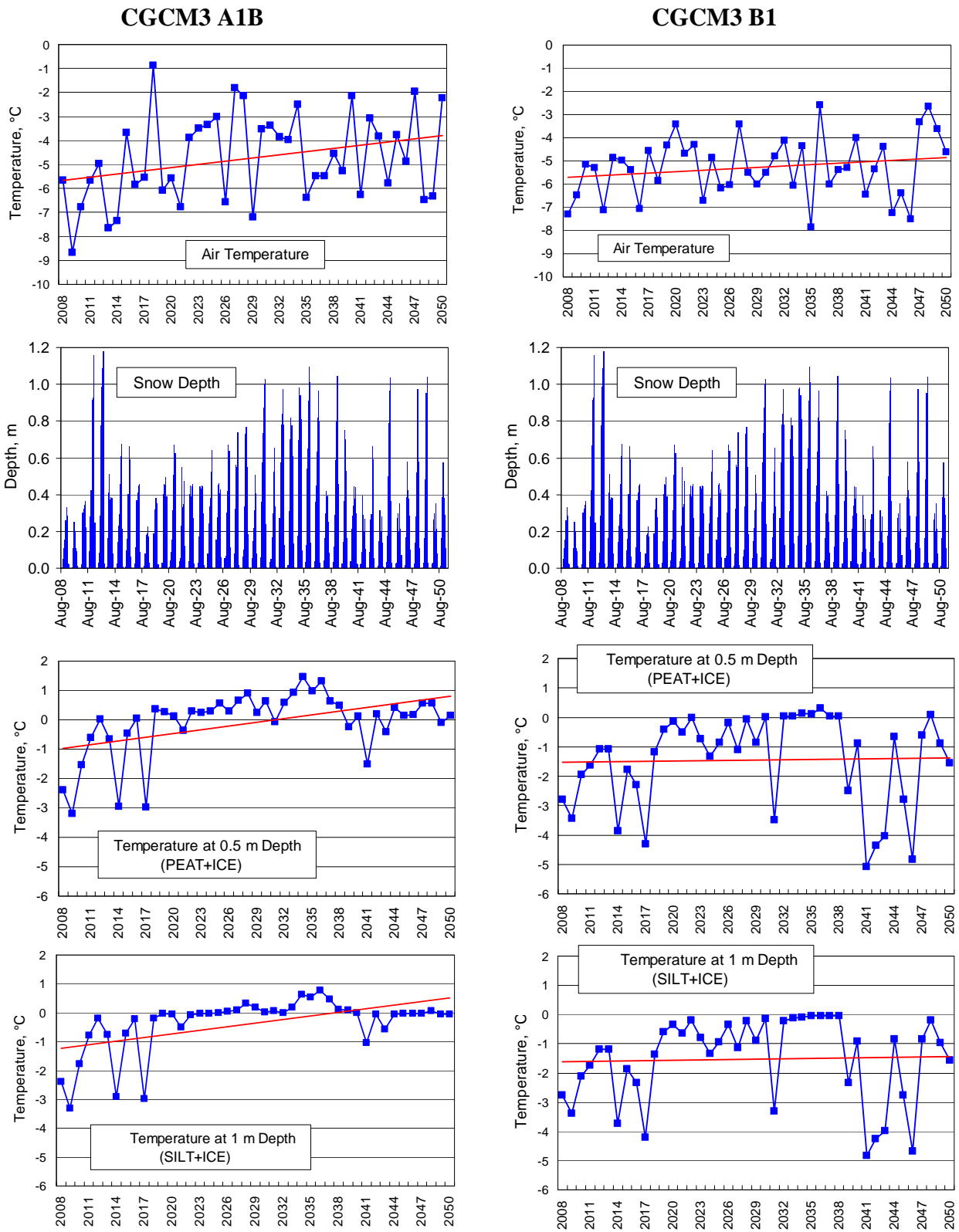


Figure 10. Modeled (CCCma CGCM3) mean annual air temperature and Modeled (GIPL) mean annual soil temperature dynamics for the natural conditions at the Kiniktuaraq AP-06 site during 2008-2050 using CCCma CGCM3 **A1B** and **B1** forcing scenario with historical (observed) data on the snow depth.

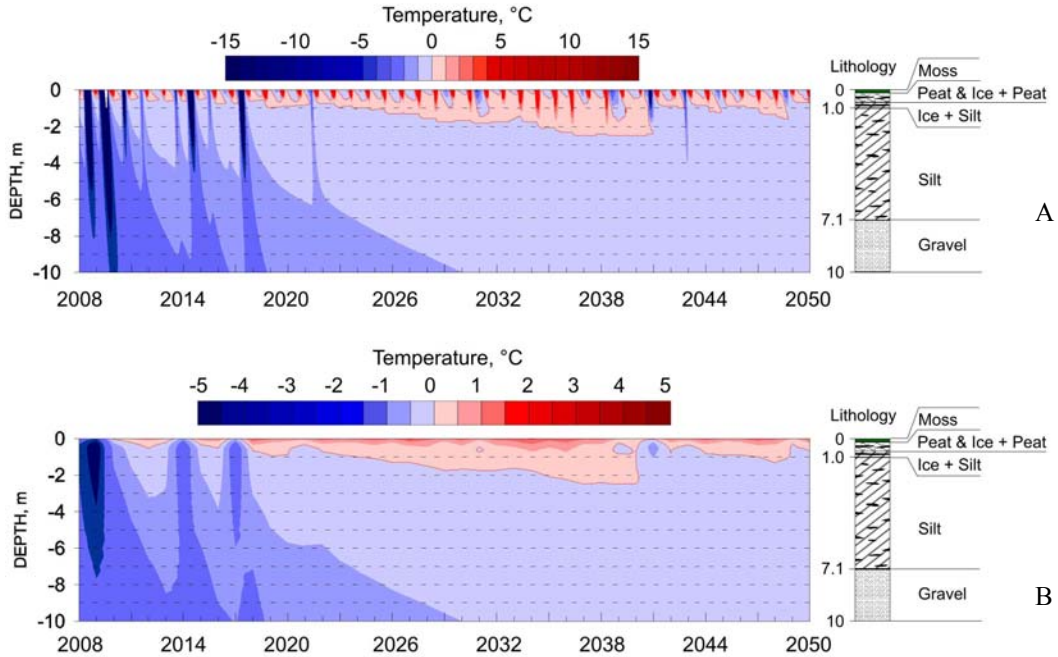


Figure 11. Modeled seasonal (A) and mean annual (B) permafrost temperature field dynamics for the natural conditions at the Kiniktuuraq AP-06 proposed relocation site during 2008-2050 using CCCma CGCM3 **A1B** forcing scenario with historical (observed) data on the snow depth.

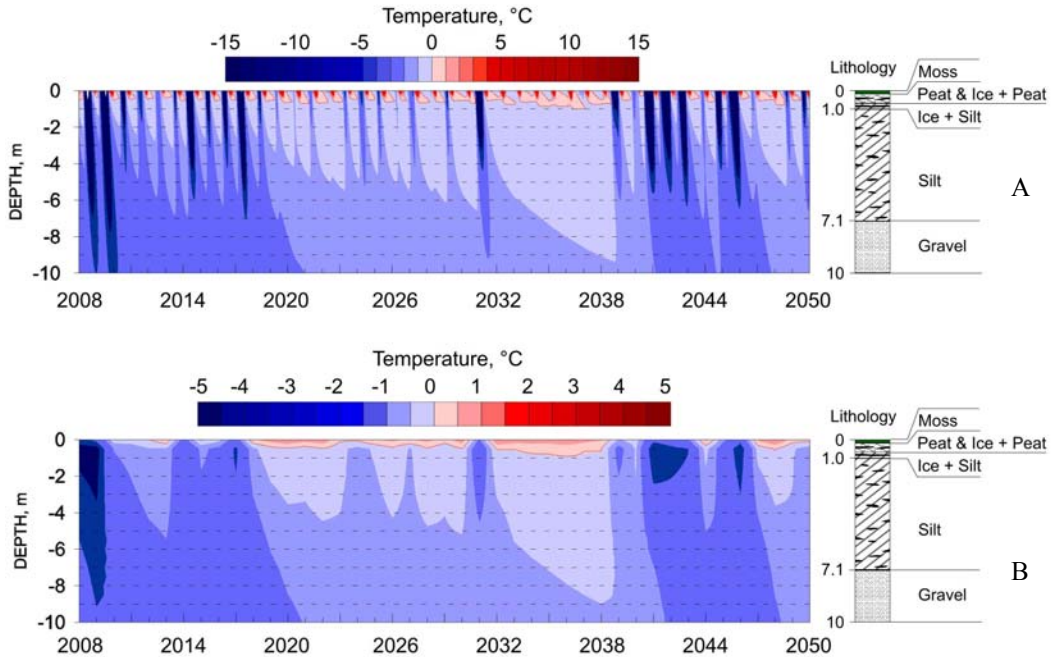
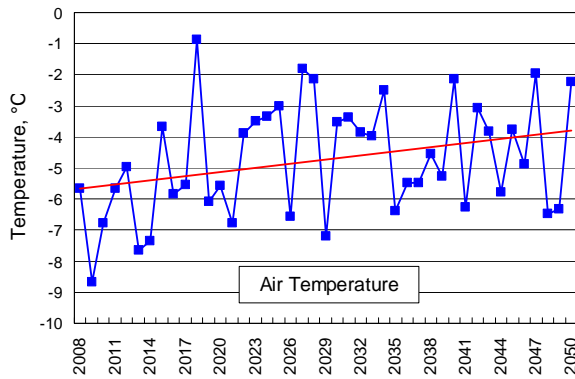


Figure 12. Modeled (GIPL) seasonal (A) and mean annual (B) permafrost temperature field dynamics for the natural conditions at the Kiniktuuraq AP-06 proposed relocation site during 2008-2050 using CCCma CGCM3 **B1** forcing scenario with historical (observed) data on the snow depth.

CGCM3 A1B



CGCM3 B1

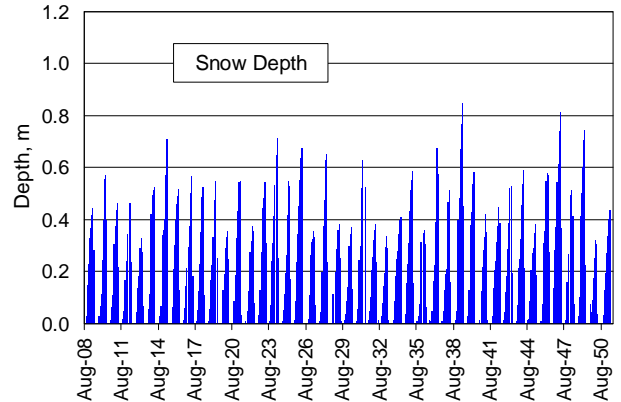
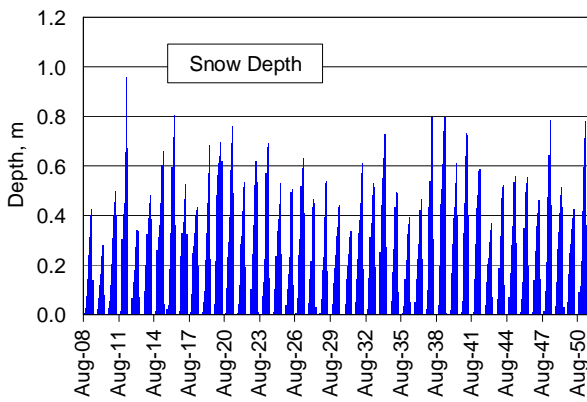
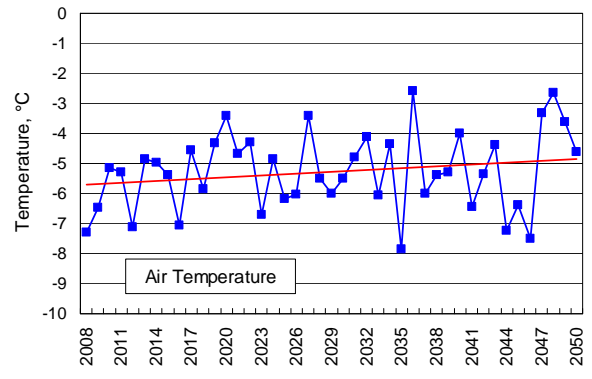


Figure 13. Modeled (CCCma CGCM3 **A1B** and **B1** scenarios) mean annual air temperature and snow depth, which have been using for the (GIPL) simulation of permafrost temperature dynamics for the case with modified surface conditions (gravel fill, silt + gravel cap) at the Kiniktuaraq AP-06 proposed relocation site during 2008-2050.

6 ft Gravel Fill

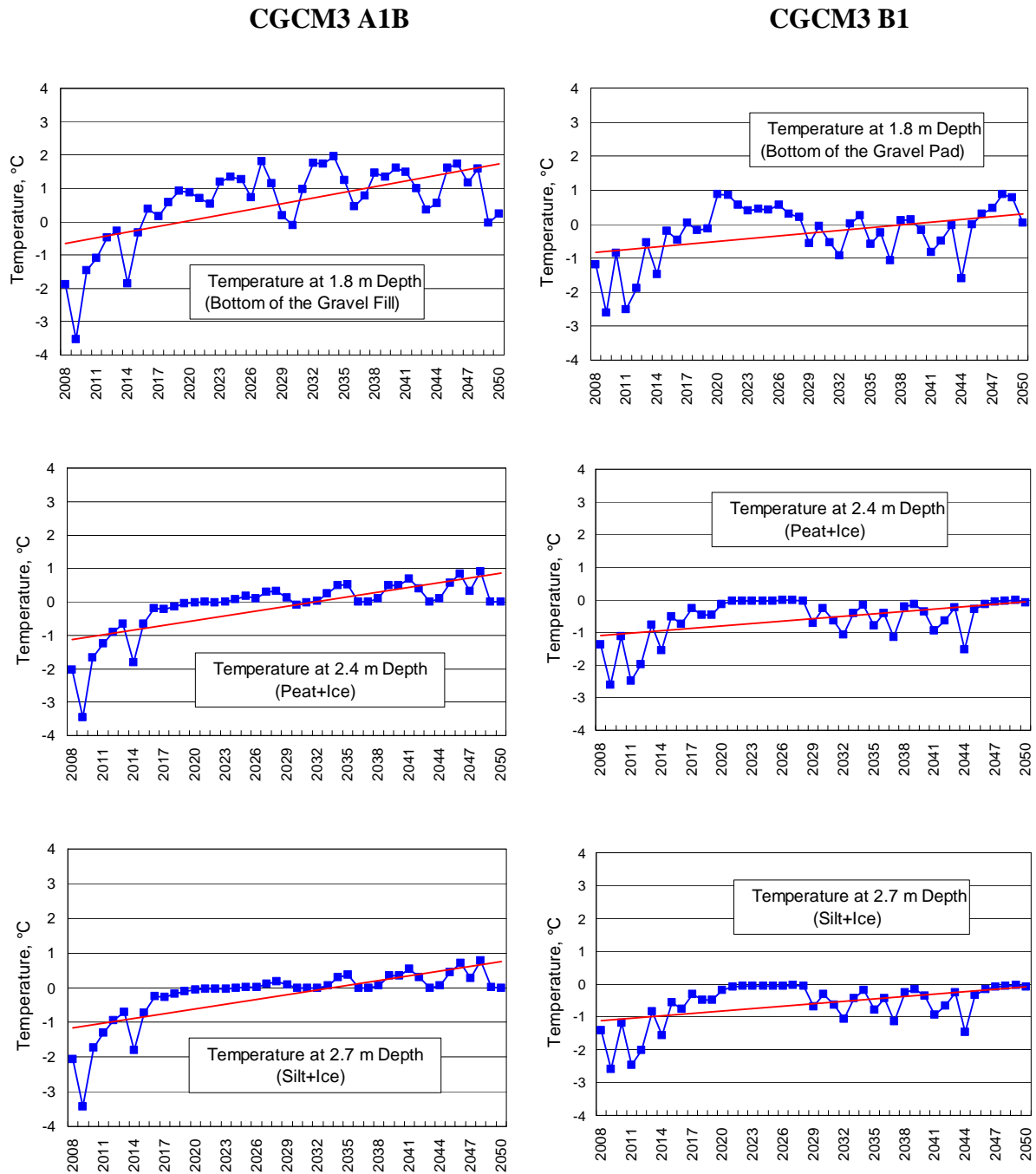


Figure 14. Modeled (GIPL) series of mean annual permafrost temperature for the case with 6 feet/1.8 m gravel fill at the Kiniktuaraq AP-06 proposed relocation site during 2008-2050 using CCCma CGCM3 A1B and B1 forcing scenarios .

6 ft Gravel Fill

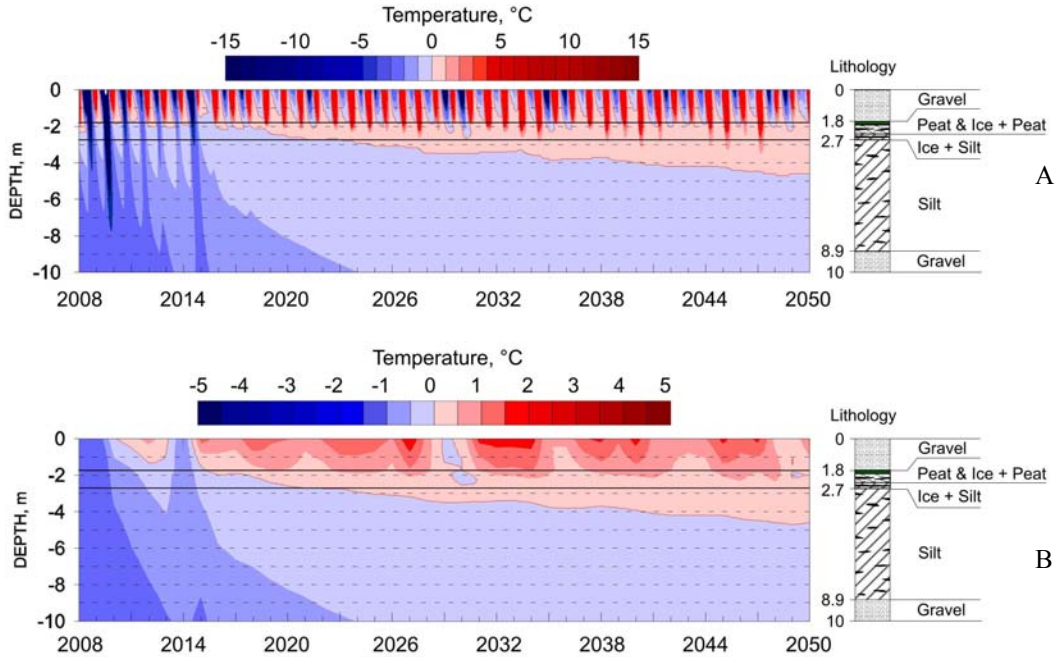


Figure 15. Modeled (GIPL) seasonal (A) and mean annual (B) permafrost temperature field dynamics for the case with 6 feet/1.8 m gravel fill at the Kiniktuuraq AP-06 proposed relocation site during 2008-2050 using CCCMA GCM **A1B** forcing scenario.

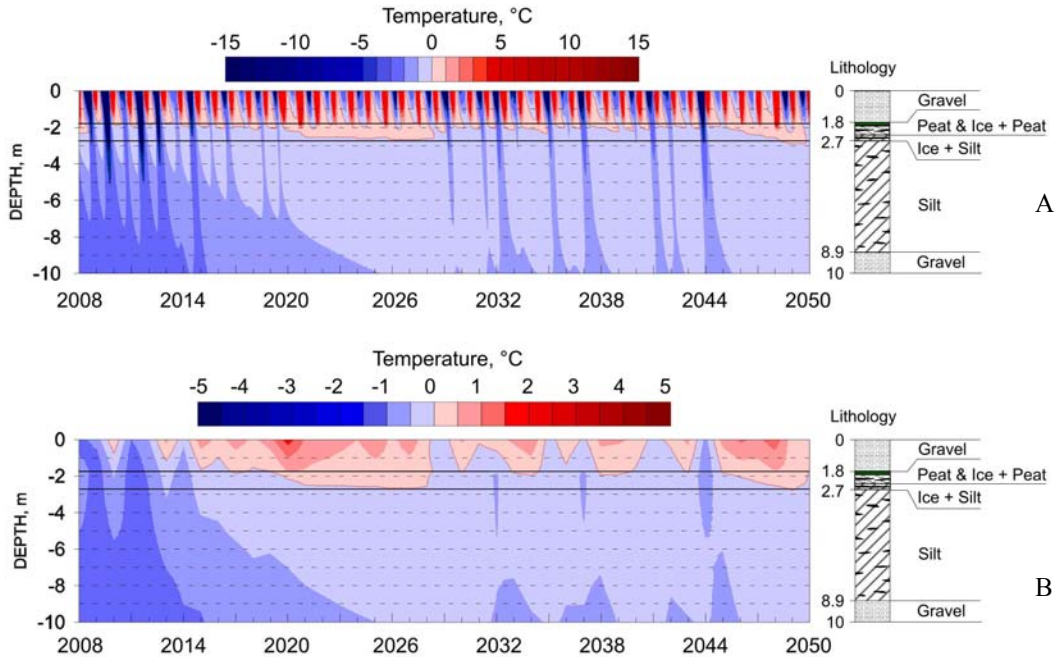


Figure 16. Modeled (GIPL) seasonal (A) and mean annual (B) permafrost temperature field dynamics for the case with 6 feet/1.8 m gravel fill at the Kiniktuuraq AP-06 proposed relocation site during 2008-2050 using CCCMA GCM **B1** forcing scenario.

9 ft Gravel Fill

CGCM3 A1B

CGCM3 B1

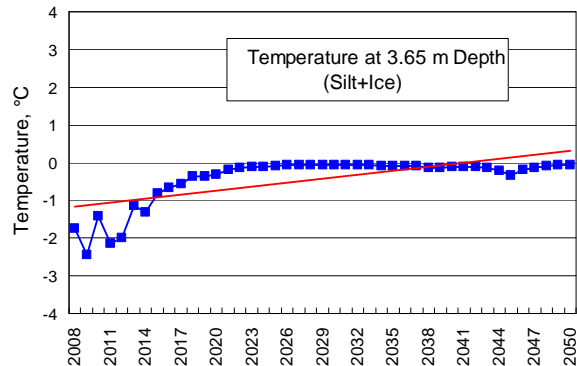
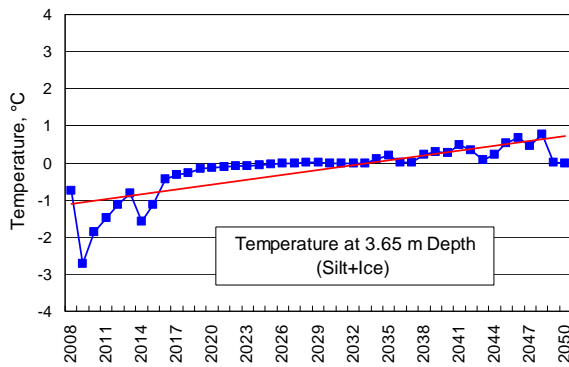
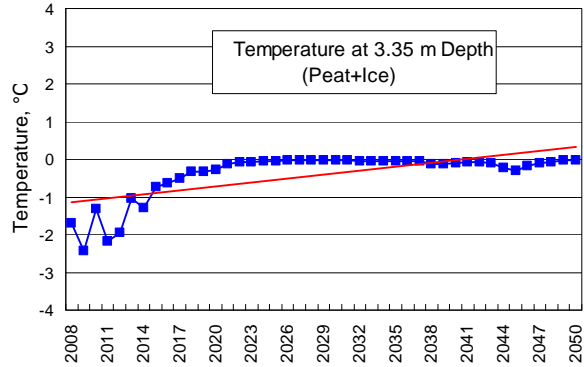
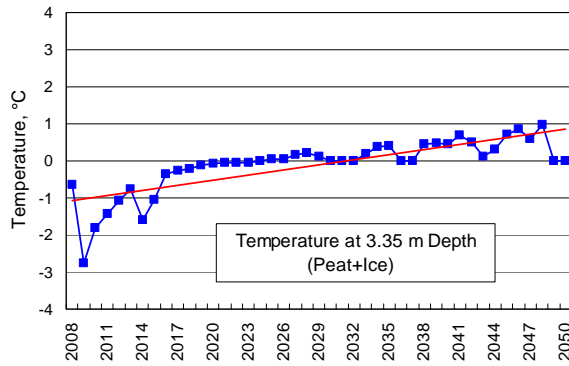
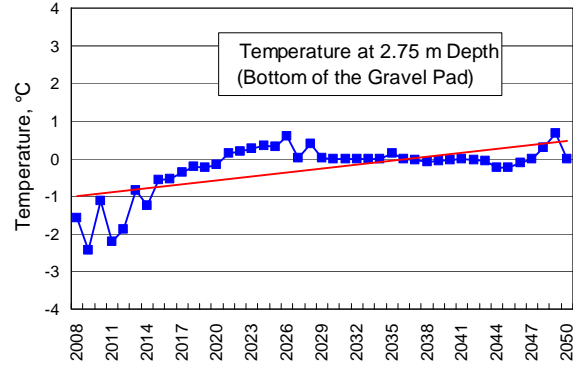
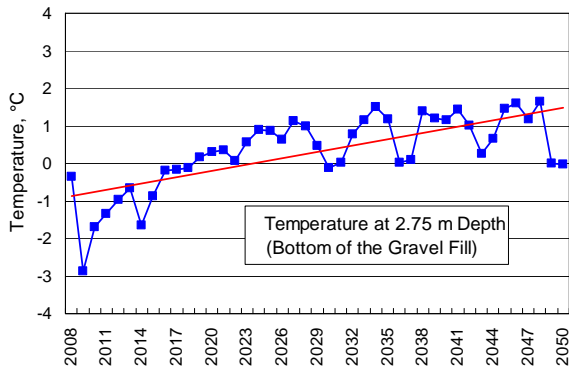


Figure 17. Modeled (GIPL) series of mean annual permafrost temperature for the case with 9 feet/2.75 m gravel fill at the Kiniktuaraq AP-06 proposed relocation site during 2008-2050 using CCCma CGCM3 **A1B** and **B1** forcing scenarios.

9 ft Gravel Fill

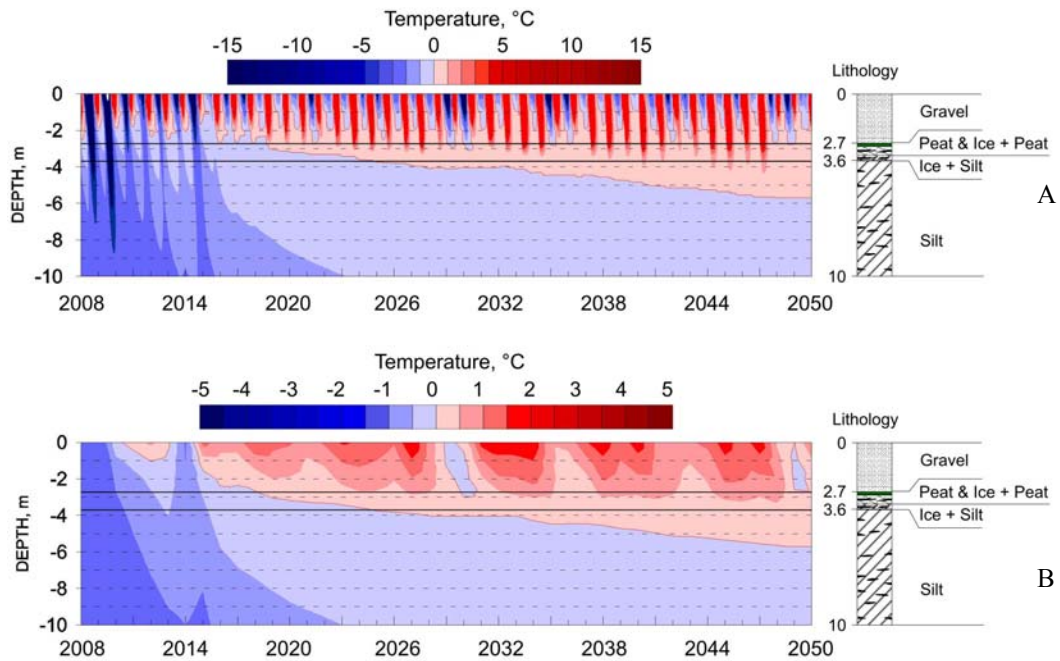


Figure 18. Modeled (GIPL) seasonal (A) and mean annual (B) permafrost temperature field dynamics for the case with 9 feet/2.75 m gravel fill at the Kiniktuuraq AP-06 proposed relocation site during 2008-2050 using CCCma CGCM3 **A1B** forcing scenario.

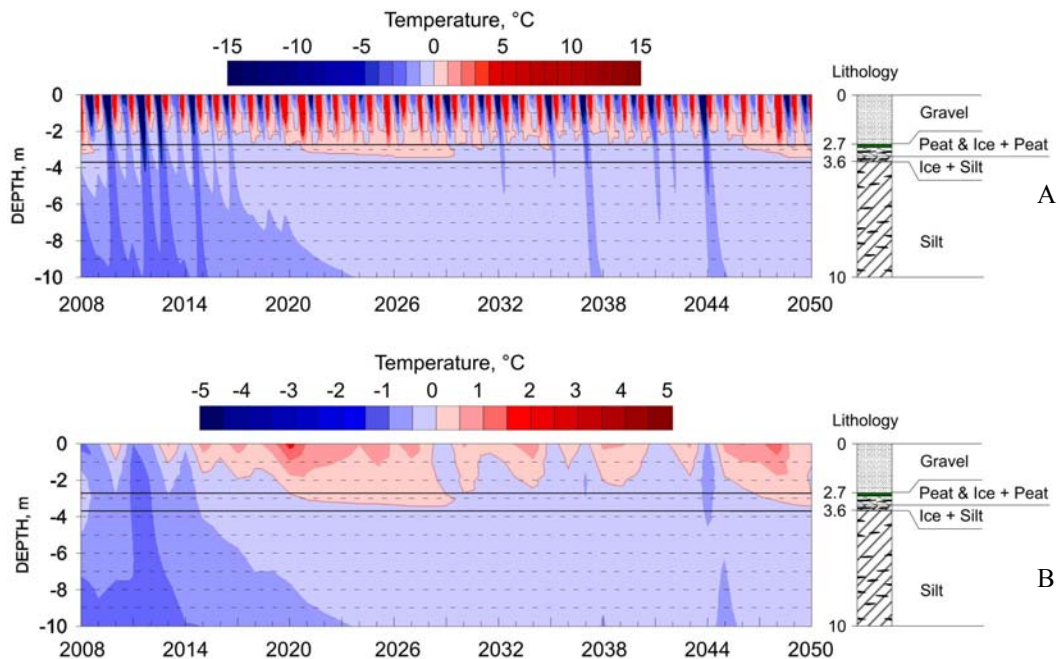
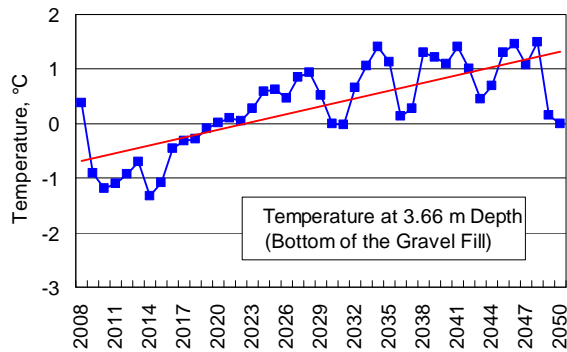


Figure 19. Modeled (GIPL) seasonal (A) and mean annual (B) permafrost temperature field dynamics for the case with 9 feet/2.75 m gravel fill at the Kiniktuuraq AP-06 proposed relocation site during 2008-2050 using CCCma CGCM3 forcing **B1** scenario.

12 ft Gravel Fill

CGCM3 A1B



CGCM3 B1

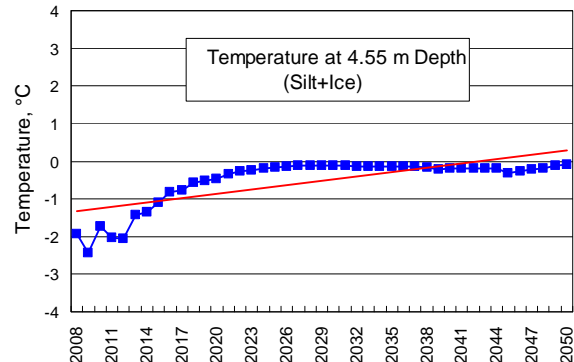
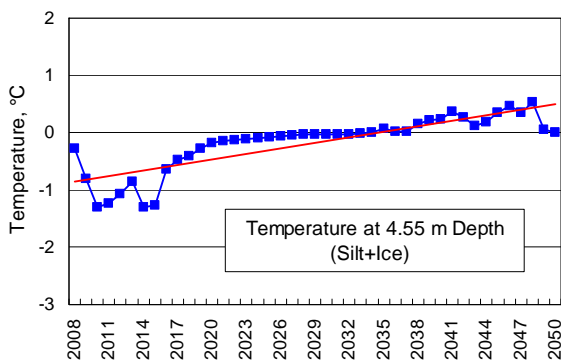
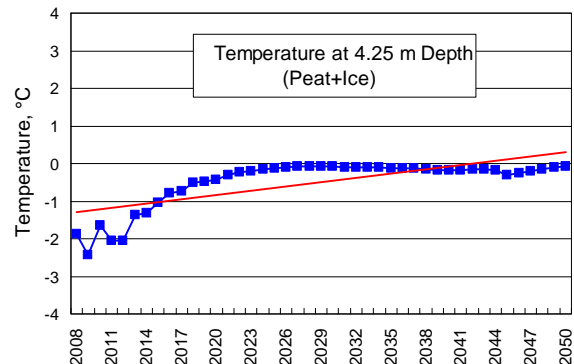
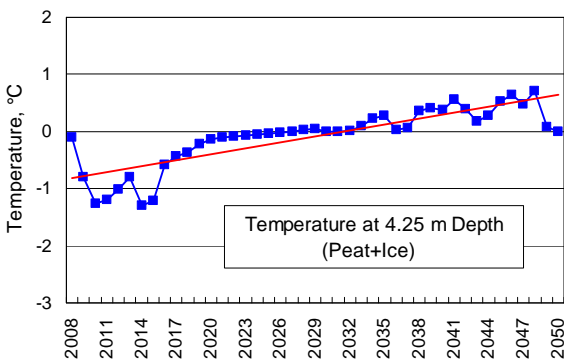
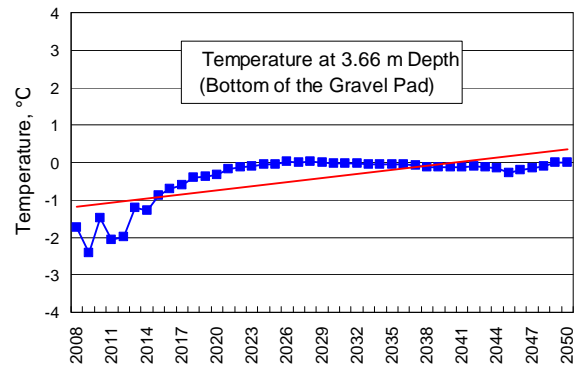


Figure 20. Modeled (GIPL) permafrost temperature dynamics for the case with 12 feet/3.65 m gravel fill at the Kiniktuaraq AP-06 proposed relocation site during 2008-2050 using CCCma CGCM3 **A1B** and **B1** forcing scenarios.

12 ft Gravel Fill

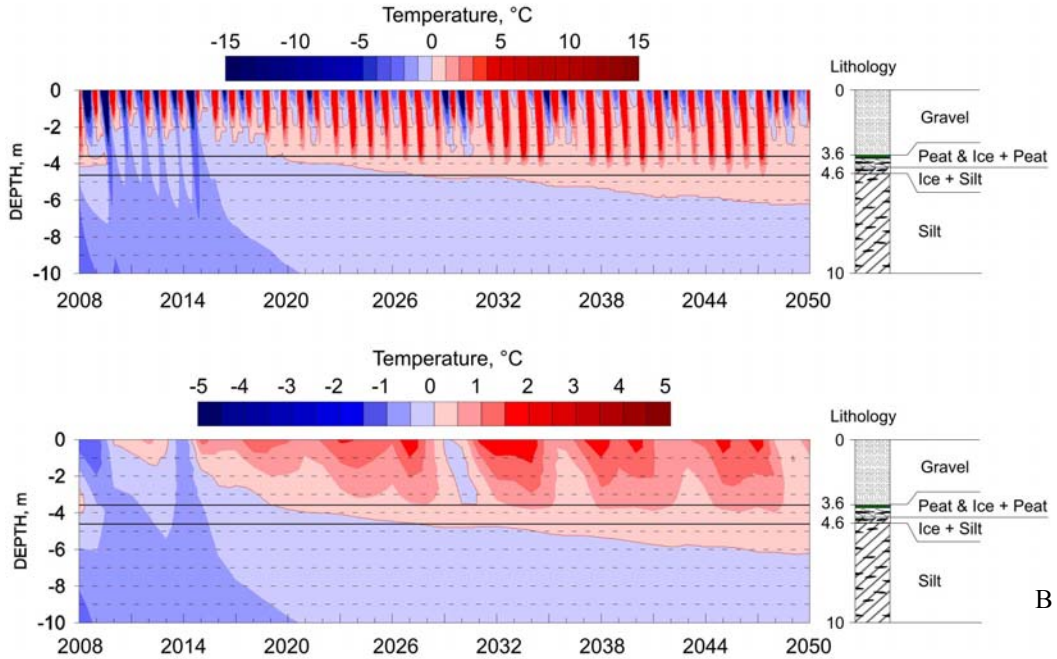


Figure 21. Modeled (GIPL) seasonal (A) and mean annual (B) permafrost temperature field dynamics for the case with 12 feet/3.66 m gravel fill at the Kiniktuuraq AP-06 proposed relocation site during 2008-2050 using CCCma CGCM3 **A1B** forcing scenario.

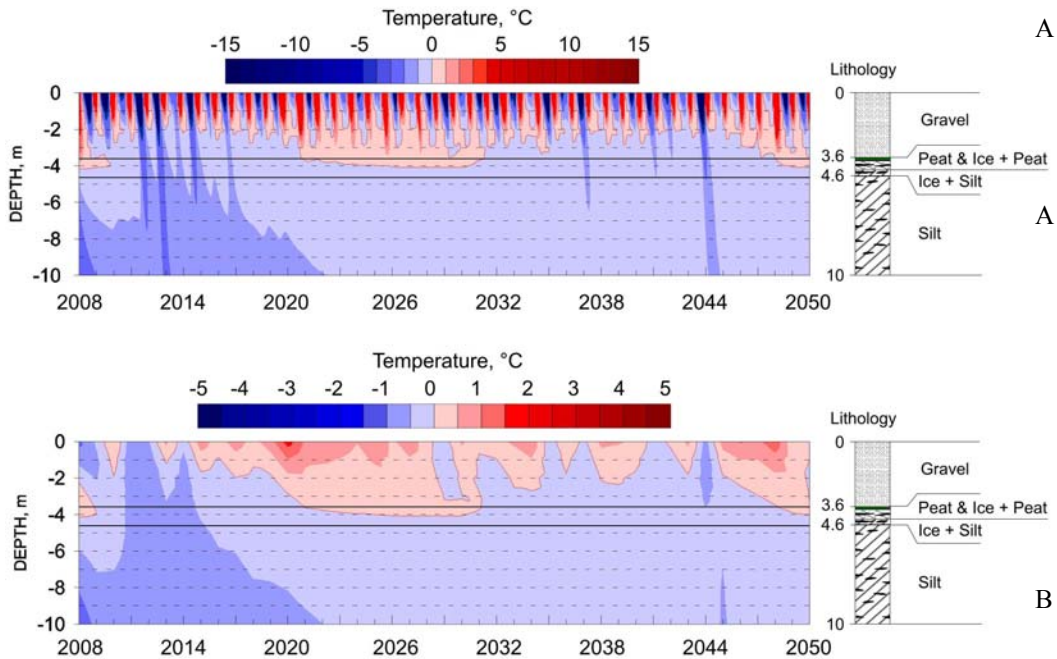


Figure 22. Modeled (GIPL) seasonal (A) and mean annual (B) permafrost temperature field dynamics for the case with 12 feet/3.66 m gravel fill at the Kiniktuuraq AP-06 proposed relocation site during 2008-2050 using CCCma CGCM3 **B1** forcing scenario.

5 ft Silt + 1 ft Gravel

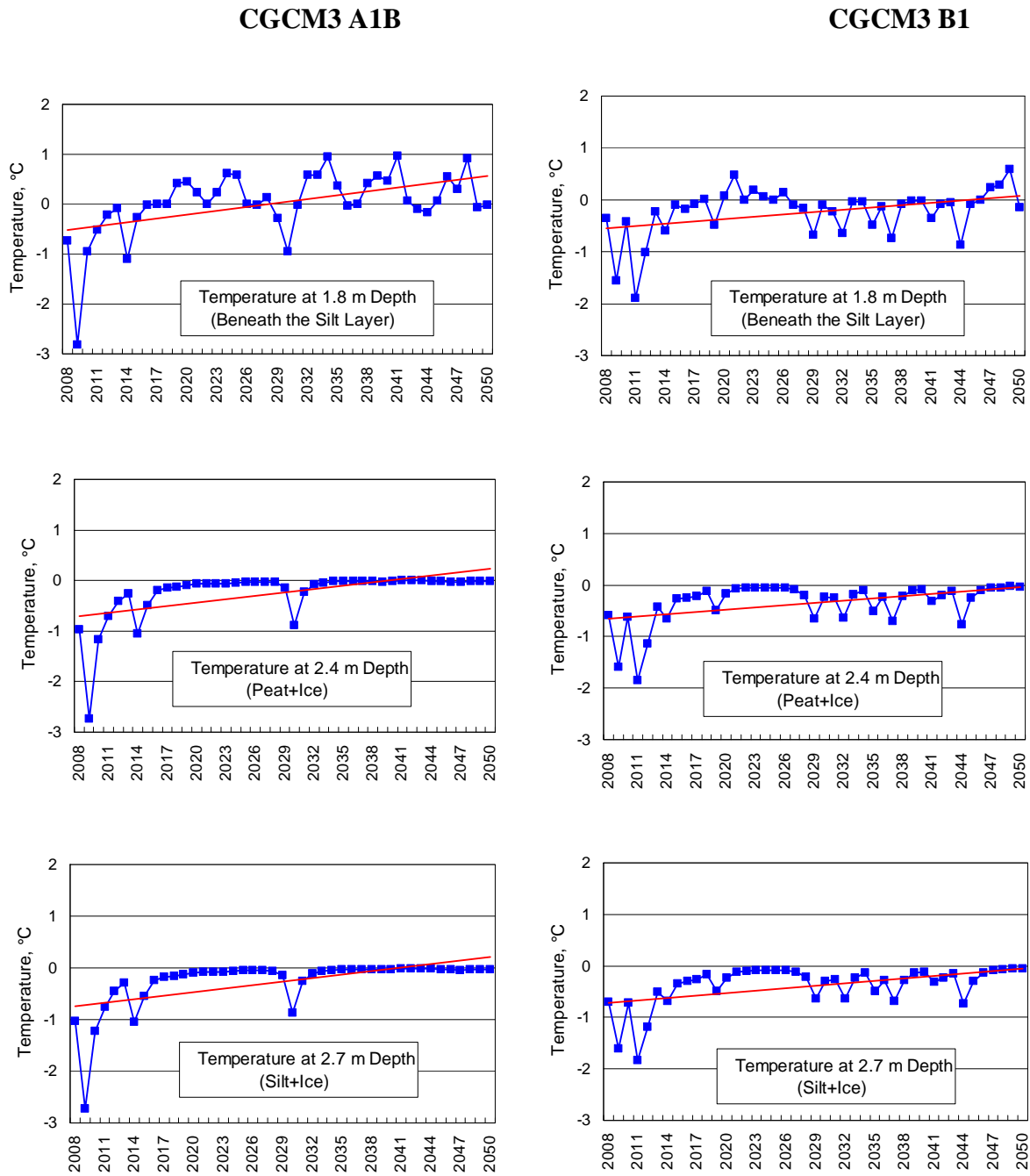


Figure 23. Modeled (GIPL) series of mean annual permafrost temperature for the case with 5 feet Silt + 1 foot gravel (1.5 m + 0.3 m gravel) at the Kiniktuaraq AP-06 proposed relocation site during 2008-2050 using CCCma CGCM3 forcing **A1B** and **B1** scenarios.

5 ft Silt + 1 ft Gravel

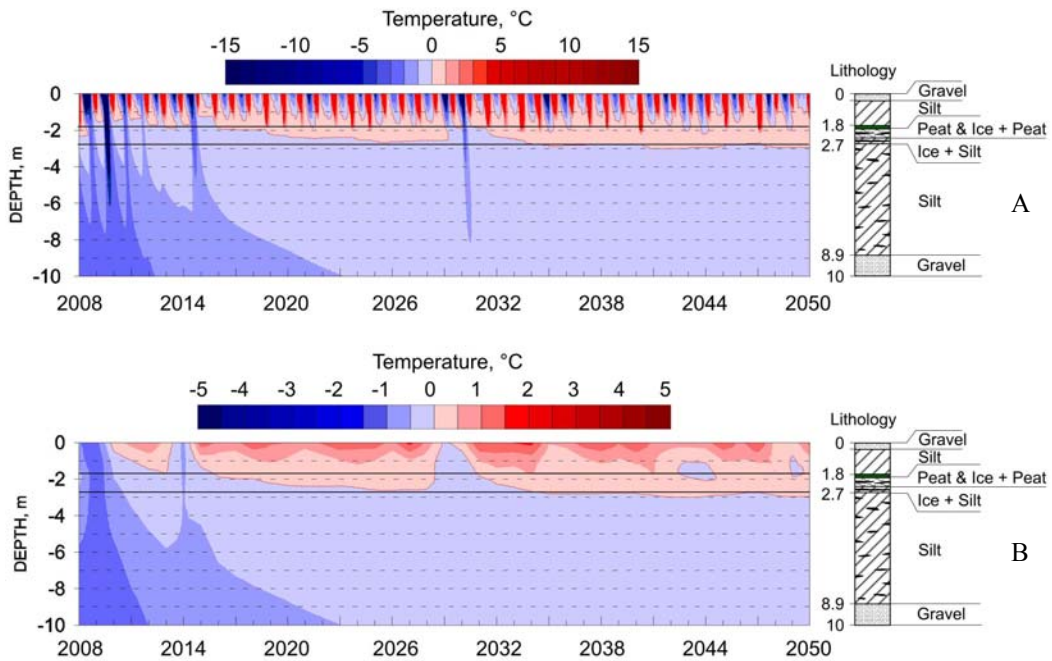


Figure 24. Modeled (GIPL) seasonal (A) and mean annual (B) permafrost temperature field dynamics for the case with 5 feet silt + 1 foot gravel (1.5 m silt + 0.3 m gravel) at the Kiniktuaraq AP-06 proposed relocation site during 2008-2050 using CCCma CGCM3 **A1B** forcing scenario.

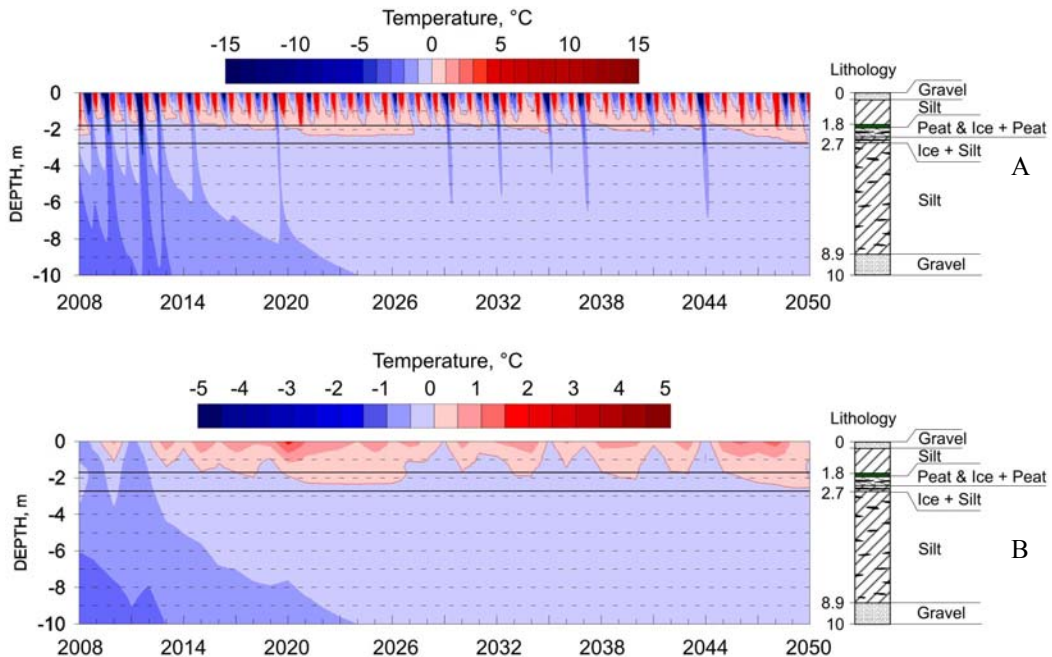


Figure 25. Modeled (GIPL) seasonal (A) and mean annual (B) permafrost temperature field dynamics for the case with 5 feet silt + 1 foot gravel (1.5 m silt + 0.3 m gravel) at the Kiniktuaraq AP-06 proposed relocation site during 2008-2050 using CCCma CGCM3 **B1** forcing scenario.

8 ft Silt + 1 ft Gravel

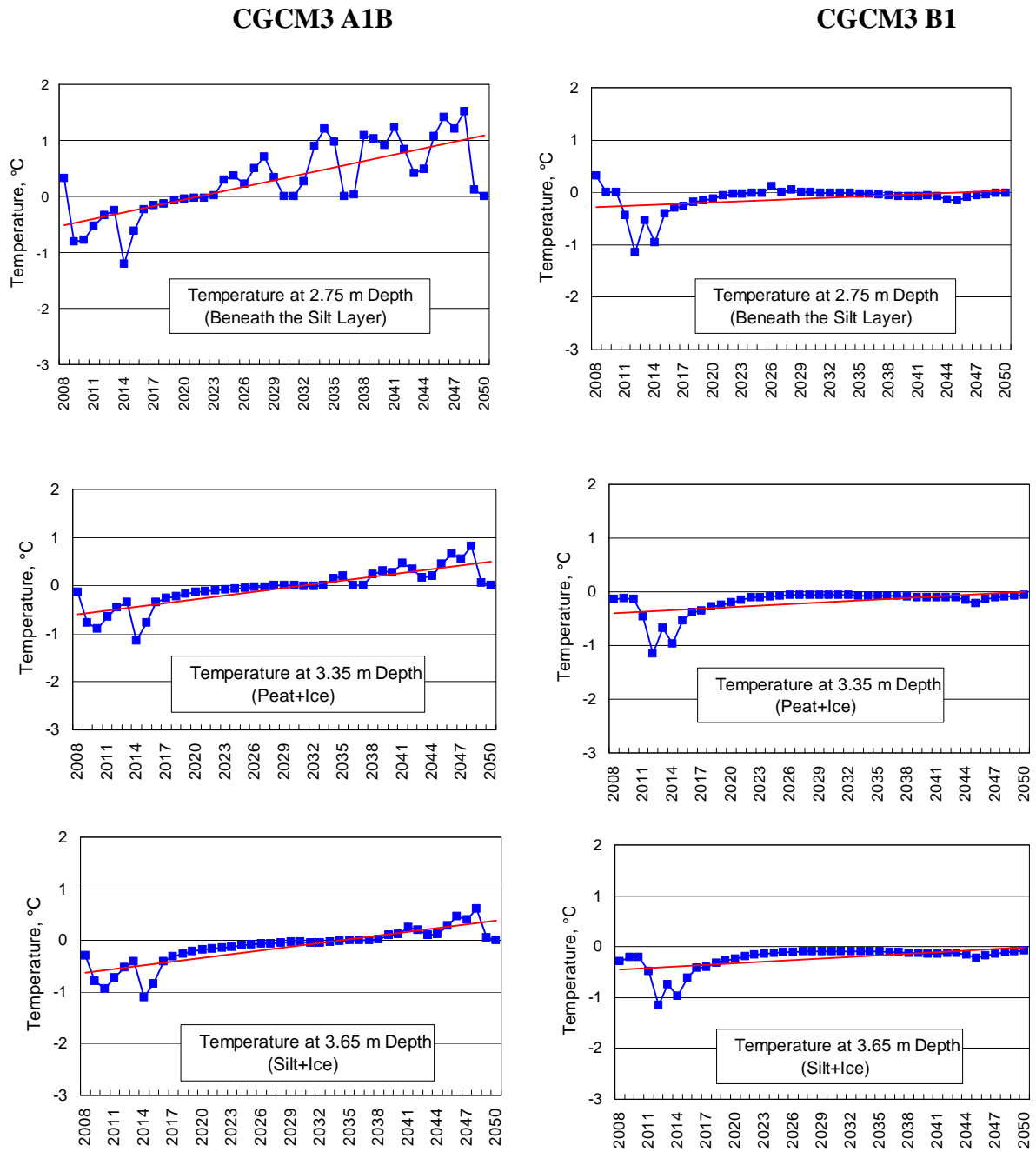


Figure 26. Modeled (GIPL) series of mean annual permafrost temperature for the case with 8 feet Silt + 1 foot gravel (2.42 m +0.3 m) at the Kiniktuaraq AP-06 proposed relocation site during 2008-2050 using CCCma CGCM3 **A1B** and **B1** forcing scenarios.

8 ft Silt + 1 ft Gravel

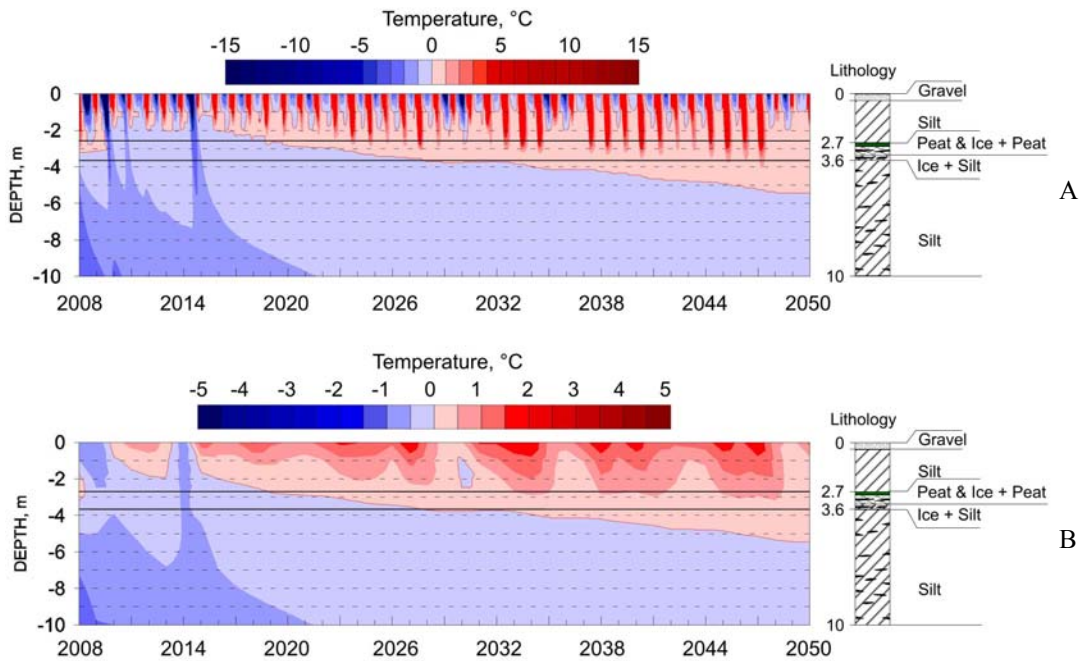


Figure 27. Modeled (GIPL) seasonal (A) and mean annual (B) permafrost temperature field dynamics for the case with 8 feet silt + 1 foot gravel (2.75 m silt + 0.3 m gravel) at the Kiniktuuraq AP-06 proposed relocation site during 2008-2050 using CCCma CGCM3 **A1B** forcing scenario.

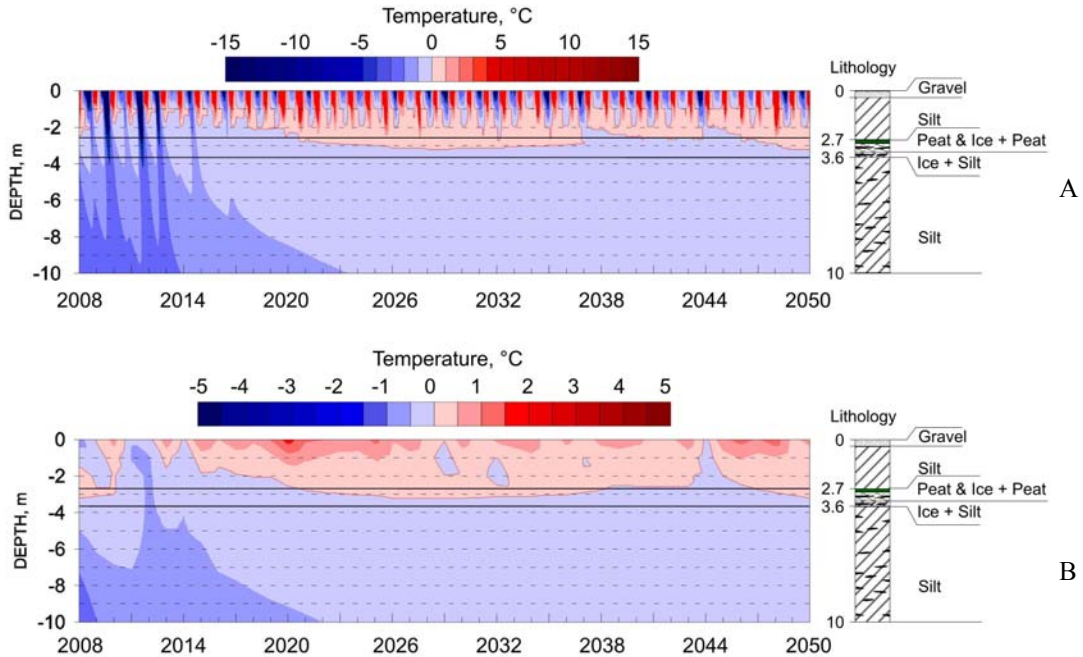


Figure 28. Modeled (GIPL) seasonal (A) and mean annual (B) permafrost temperature field dynamics for the case with 8 feet silt + 1 foot gravel (2.75 m silt + 0.3 m gravel) at the Kiniktuuraq AP-06 proposed relocation site during 2008-2050 using CCCma CGCM3 **B1** forcing scenario.

11 ft Silt + 1 ft Gravel

CGCM3 A1B

CGCM3 B1

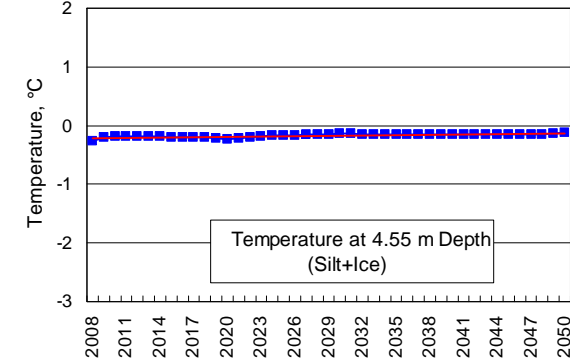
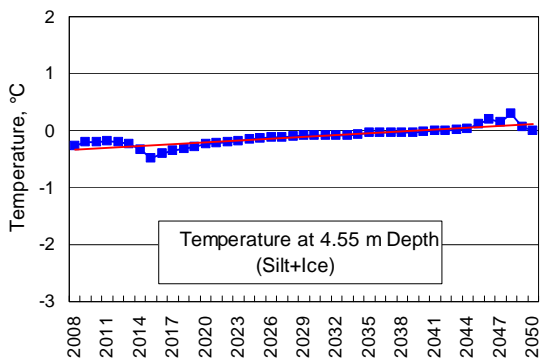
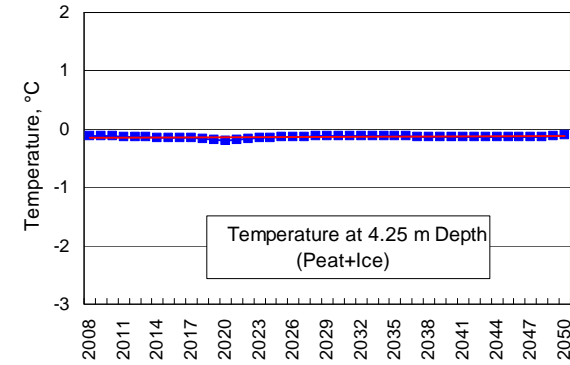
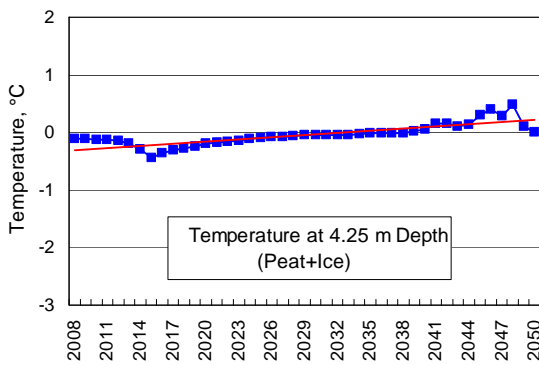
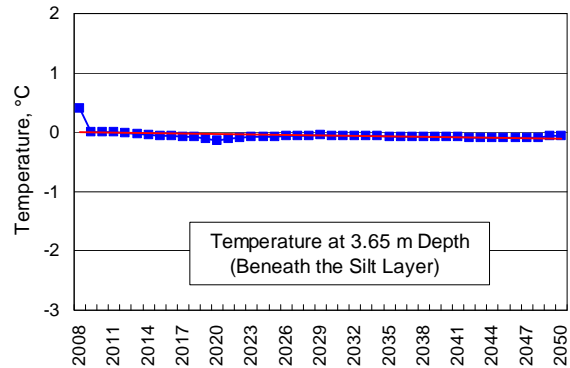
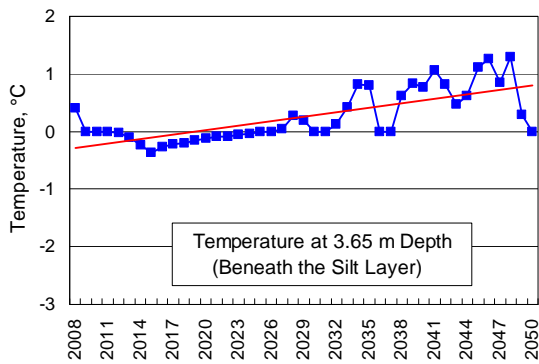


Figure 29. Modeled (GIPL) series of mean annual permafrost temperature for the case with 11 feet Silt + 1 foot gravel cap (3.35 m +0.3 m) at the Kinikturaq AP-06 proposed relocation site during 2008-2050 using CCCma CGCM3 **A1B** and **B1** forcing scenarios.

11 ft Silt + 1 ft Gravel

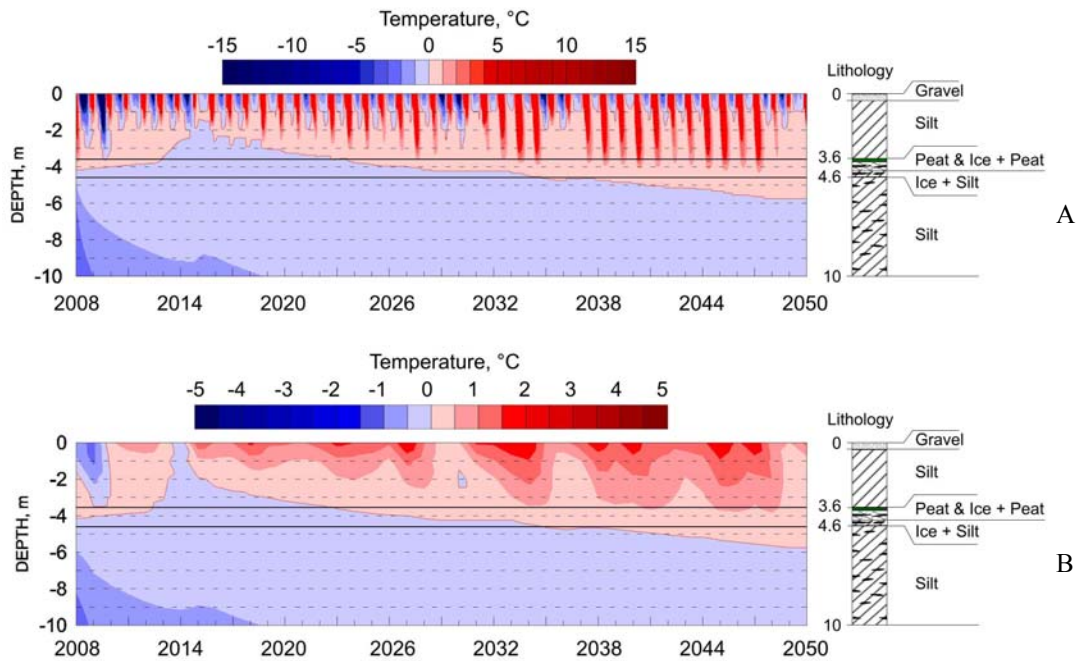


Figure 30. Modeled (GIPL) seasonal (A) and annual (B) permafrost temperature field dynamics for the case with 11 feet silt + 1 foot gravel cap (3.35 m silt + 0.3 m gravel) at the Kiniktuaraq AP-06 proposed relocation site during 2008-2050 using CCCma CGCM3 **A1B** forcing scenario.

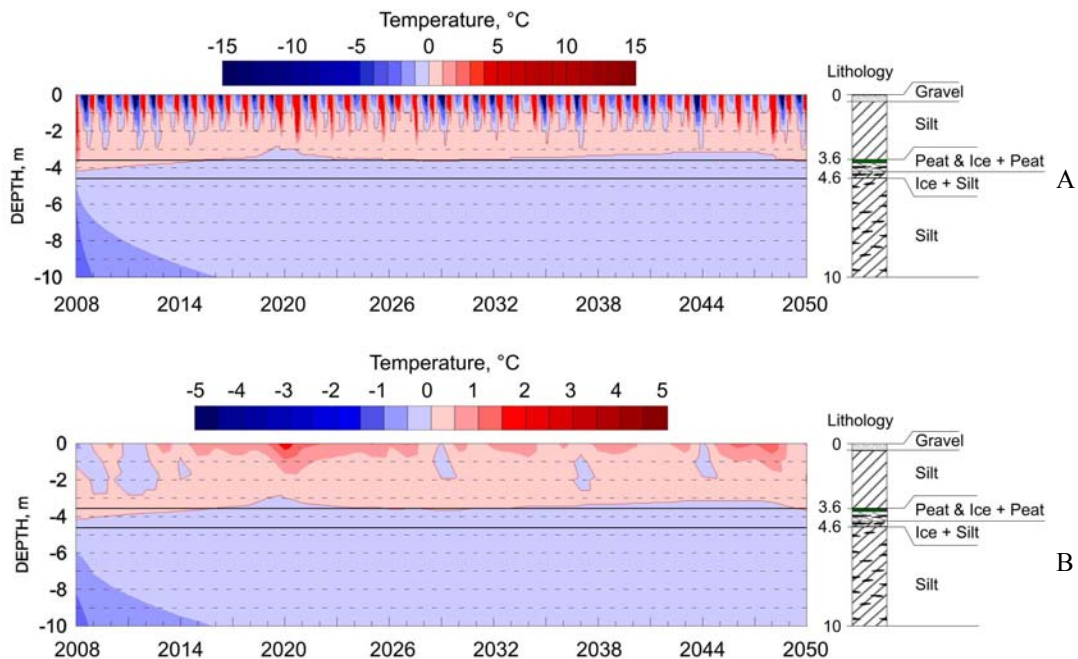


Figure 31. Modeled (GIPL) seasonal (A) and annual (B) permafrost temperature field dynamics for the case with 11 feet silt + 1 foot gravel cap (3.35 m silt + 0.3 m gravel) at the Kiniktuaraq AP-06 proposed relocation site during 2008-2050 using CCCma CGCM3 **B1** forcing scenario

12 ft Gravel Fill

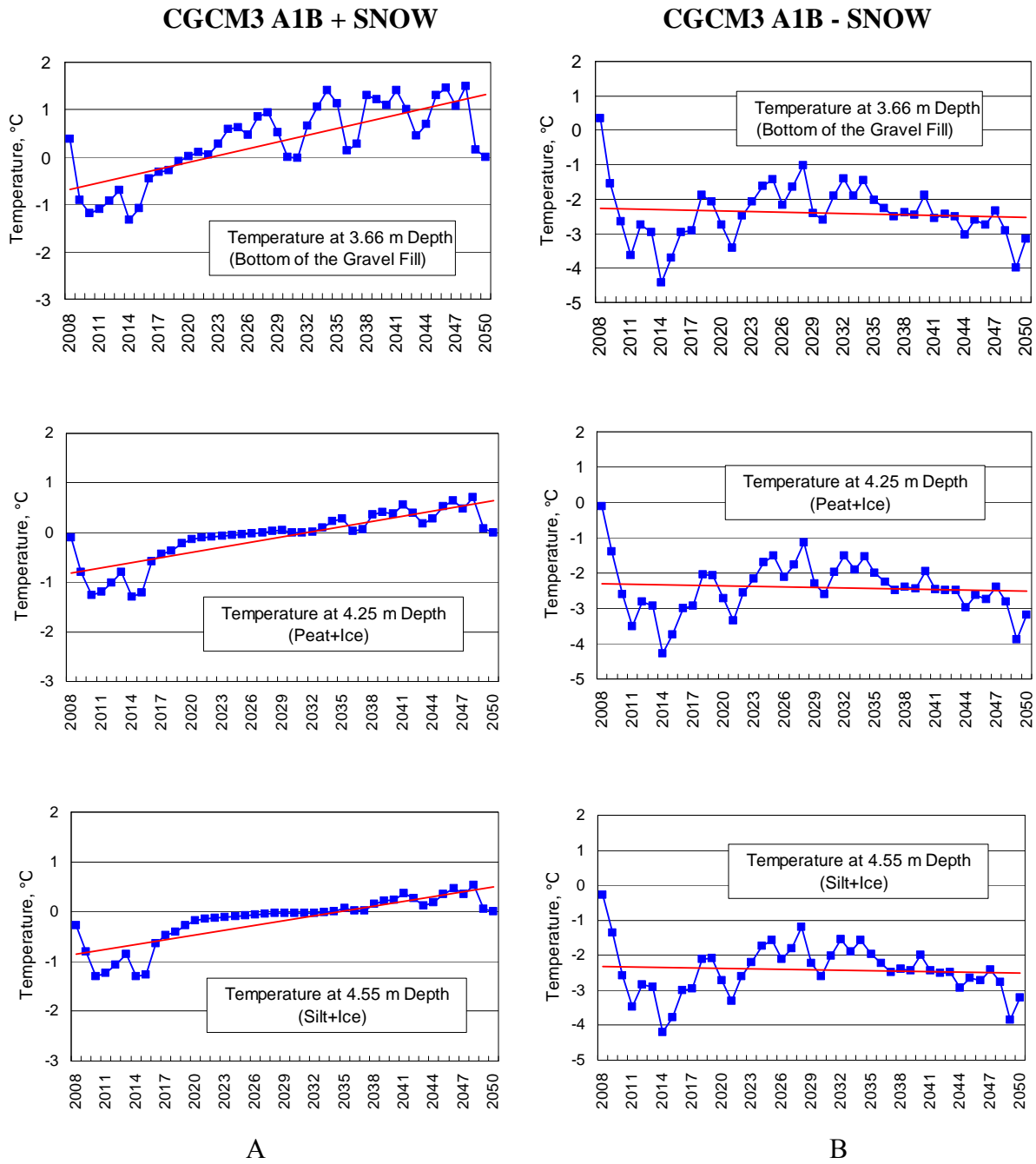


Figure 32. A - Modeled (GIPL) permafrost temperature dynamics for the case with 12 feet/3.65 m gravel fill at the Kiniktuuraq AP-06 proposed relocation site during 2008-2050 using CCCma CGCM3 A1B forcing scenario. B - Modeled (GIPL) permafrost temperature dynamics for the case with 12 feet/3.65 m gravel fill at the Kiniktuuraq AP-06 proposed relocation site during 2008-2050 using CCCma CGCM3 A1B forcing scenario with removing snow cover simulation (snow depth does not exceed 0.1 m).

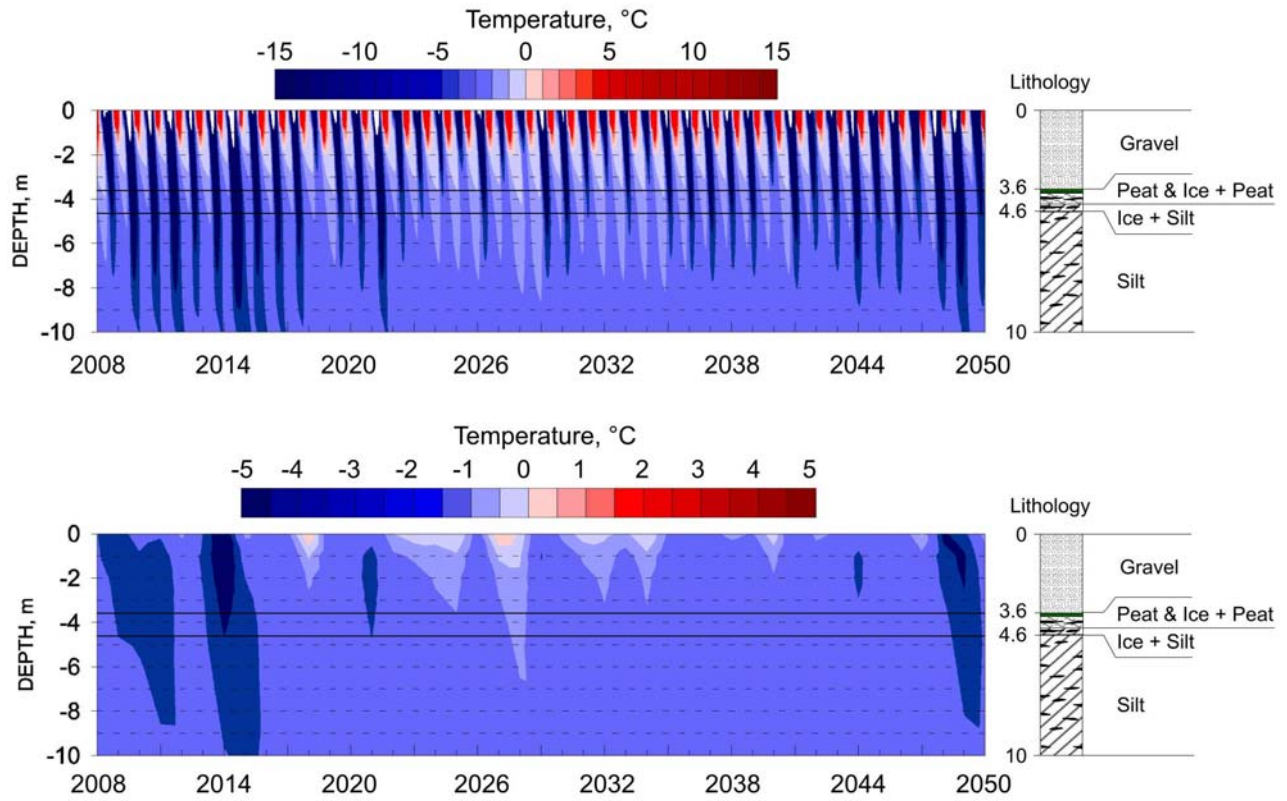


Figure 33. Modeled (GIPL) permafrost temperature dynamics for the case with 12 feet/3.65 m gravel fill at the Kiniktuuraq AP-06 proposed relocation site during 2008-2050 using CCCma CGCM3 **A1B** forcing scenario with removing snow cover simulation (snow depth does not exceed 0.1 m).